

DX-LGSW INTEGRATION REPORT

Doc. No. ARGOS Tech Note 120
 Issue 2
 Date 30/01/2014

Prepared	L. Busoni, M. Bonaglia, T. Mazzoni, S. Esposito	2014/01/30
	Name	Date
Approved	N. Surname	yyyy/mm/dd
	Name	Date
Released	N. Surname	yyyy/mm/dd
	Name	Date



TABLE OF CONTENTS

Change Record.....4

1 Scope.....4

2 Applicable documents.....4

3 LGSW unit requirement5

4 LGSW description.....6

5 Definitions.....8

6 Wavefront sensing.....9

6.1 Spatial sampling9

6.2 Spots geometry on CCD9

6.3 Frame rate.....10

6.4 Read-out Noise.....10

6.5 Common Mode Noise residual.....11

6.6 Wavefront sensor measurement error.....11

6.7 Slope computation.....12

6.8 Slope RMS.....12

7 Gating units.....14

8 Sending and receiving slopes.....15

9 Tip Tilt Unit.....17

10 pnCCD frame grabbing and processing18

11 Slope offset.....19

12 Pupil Stabilization20

13 Jitter Stabilization22

13.1 Tilt estimate accuracy22

13.2 Piezo Mirror Commands23

13.3 Dynamical performances24

14 LGS spot size estimation algorithm24

15 Wavefront focus estimation algorithm24

16 Acquisition cameras.....25

17 Cooling and dry air circuits.....25

18 Internal sources and external sources.....25

19 Storing and management of calibration27

20 Diagnostic and telemetry27

20.1 Real-time data from LGSW BCU27

20.2 Snapshot.....28

20.3 Telemetry and monitoring.....28

21 Safety29

22 Maintenance31

22.1 Twiki.....31

22.2 Spare parts31

22.3 Proprietary software tools.....31

23 Appendix A - Gravity test.....32

24 Appendix B - Thermal Cycling34

24.1 Devices functionality at low temperature34

24.2 Optomechanical stability of Wavefront Sensor during thermal cycles.....36

24.3 Thermocamera measurements37

25 Appendix C - Closed loop tests with MEMS DM.....41

25.1 Use of MEMS DM to mimic the LBT-ASM42

25.2 Interaction Matrix acquisition43



DX-LGSW integration report

Doc: ARGOS Tech Note 120
Issue 2
Date 30/01/2014
Page 3 of 50

25.3 WFS measurement noise 44
25.4 Closed loop performances 45
26 Appendix D - Device list and present configuration..... 47
27 Appendix E - Spare parts list 48
28 List of acronyms..... 49



Change Record

Issue	Date	Section/ Paragraph Affected	Reasons / Remarks	Name
0.0	19.12.2013	all	created	Busoni
1.0	20.01.2014	all	major update	Busoni
2.0	30.01.2014	all		Busoni

1 Scope

This technical note describes the pre-shipping status of the DX-LGSW unit. It contains information about functionality, performances, software interfaces, diagnostic and maintenance and collects the knowledge of the LGSW gathered during its integration.

2 Applicable documents

No.	Title	Number & Issue
AD 1	ARGOS_FDR_015b_WFS "Wavefront sensor design"	3.0
AD 2	ARGOS_PDR_008 "Wavefront Sensor"	1.5
AD 3	ARGOS_PDR_005 "System Design"	1.0 29/05/2009
AD 4	Requirements fro the ARGOS BCU	1.3 - Sep, 8 2010
AD 5	Laboratory characterization of the ARGOS Laser WFS	Proc SPIE 8447 (2012) 84476B
AD 6	Gilles Orban de Xivry - PhD thesis	
AD 7	ARGOS technical note 116	
AD 8	ARGOS_FDR_003 "Top Level Requirements"	1.0 - 09/02/2010



3 LGSW unit requirement

The LGSW is designed to implement the following features:

1. Measure the wavefront x and y slope of each of the 3 laser beams with a sampling of 15x15 subapertures at a frame rate of 1kHz.
2. Range-gate the backscattered laser beams.
3. Act as frame-grabber for the pnCCD and implement the required frame corrections.
4. Collect slopes from the other ARGOS WFSs (Quad Cell TipTiltUnit and PyrWFS) and transmit them to the ASM via the Fast Link optical channel.
5. Apply slope offsets to compensate the off-axis aberrations experienced by the LGS beams.
6. Acquire the LGS beams and provide to AARB the position of the beams in the LGSW field.
7. Stabilize the pupils' position on the WFS lenslet array.
8. Correct the atmospheric tip-tilt jitter on the WFS.
9. Provide to AARB the average measure of spot size and wavefront focus.
10. Store and manage calibration data.
11. Be able to operate in the LBT environment and comply with the telescope interfaces.
12. Provide information and telemetry about WFS status.

4 LGSW description

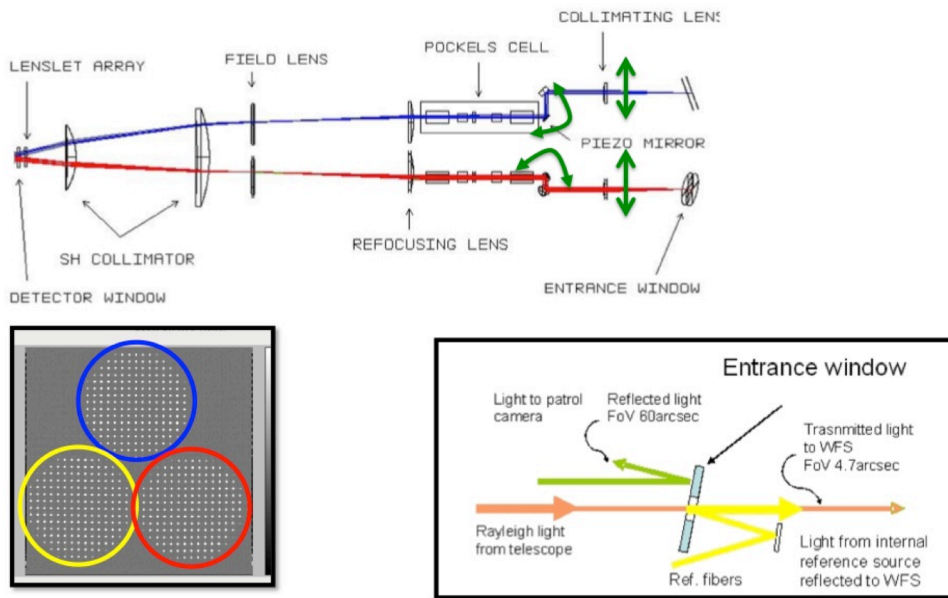


Figure 1 LGSW optical sketch. f16.6 LGS beams enter the WFS through the entrance windows (upper picture, right). The collimating lens is mounted on a XY motorized stage to act as pupil stabilizer; the tip-tilt piezo head controls the spot jitter.

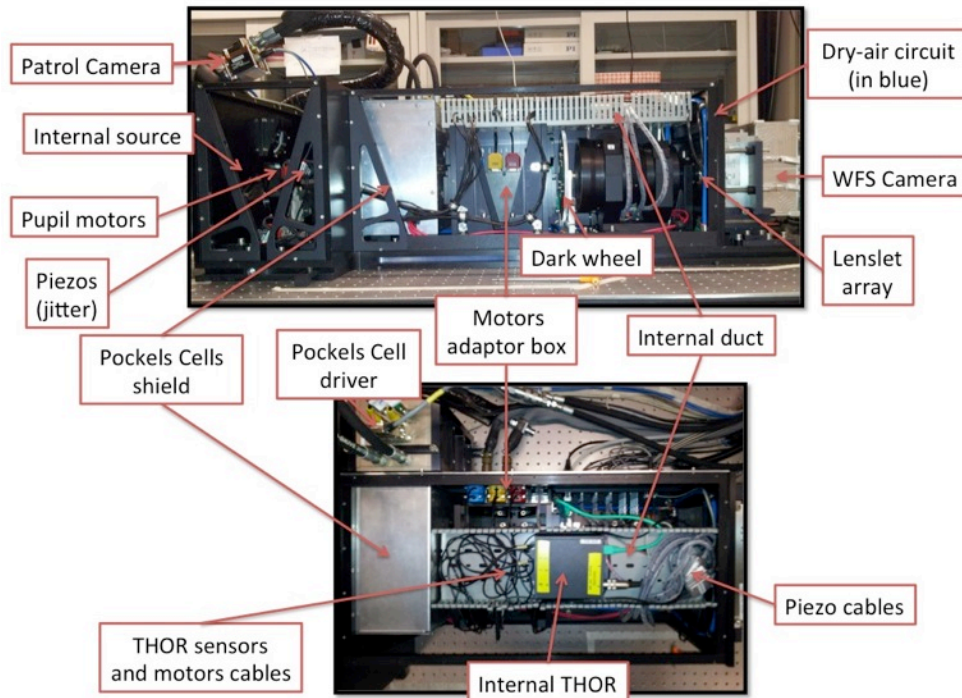


Figure 2 Internal view of the DX-LGSW

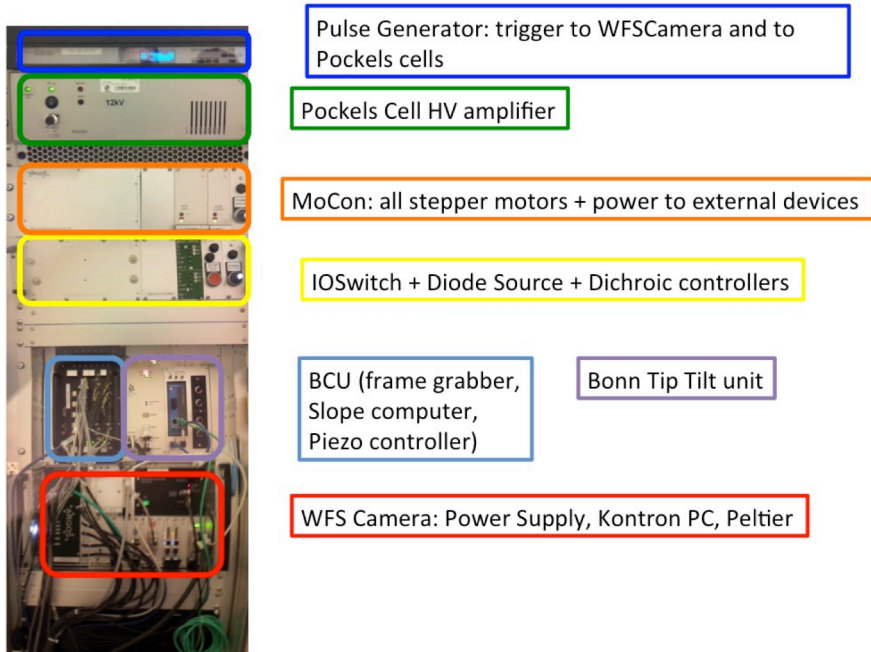


Figure 3 View of the DX-LGSW rack



5 Definitions

LGSW: the ARGOS Laser Guide Star Wavefront sensor. Includes the WFS unit, the electronic rack, the bench and all the cabling and cooling lines. It also includes the LGSW workstation and the control software.

LGSW Control SW: ensemble of all the programs that control the various bits of hardware of LGSW. The LGSW Control SW provides to the other ARGOS SW components an interface (the **LGSW Controller Client**) that must be used to operate on the LGSW (invoking commands, setting and retrieving configurations, etc....)

ARGOS Arbitrator (AARB): the software sitting at the top level of the hierarchy of the ARGOS Control SW. It controls and coordinates all the various ARGOS subsystems: LGSW, LALAS, ASM, PyrWFS, etc.

Basdard: this term is slightly mis-used in this document and identifies a twice-as-Nice SW device server. The LGSW Control SW is made (among other) of several Basdards, each devoted to controlling a specific piece of hardware.

LGSW Controller: the higher software layer in the LGSW. This program embeds a finite-state-machine to implement high-level commands like power on, setup, close-loops, etc. It coordinates the devices via the Basdards. In FLAO analogy, this is the WArbitrator.

Color convention: the 3 LGS beams have been named as "Blue", "Yellow" and "Red" and most of the cables and connector have been color-coded accordingly. See the twiki page <http://aowiki.arcetri.astro.it/ARGOSPublic/LgswChannels> for a complete description.

6 Wavefront sensing

Requirement: LGSW must provide measurements of the wavefront slopes of the 3 LGS beams. Spatial and temporal sampling and measurement noise are defined in the design documents [AD8, AD3, AD1, AD2] and translate into the following requirements: pupil sampling = 15x15 subaps, frame rate = 1kHz, measurement error = 50nm.

6.1 Spatial sampling

The external f16.6 sources (see Sect 18) produce pupil images of 15x15.25 subapertures (see Figure 4). The slight radial elongation is due to geometrical projection of the beam on the lenslet array and it is in agreement with the design (see AD2, Table 1)

6.2 Spots geometry on CCD

CCD coordinates of pupils center by FDR design are [128,190], [67, 75], [197, 75] for Blue, Red and Yellow pupil respectively (derived from AD1, Figure 7)

The critical restriction to observe is avoiding splitting subapertures between the 2 vertical halves of the CCD that are read by different read-out circuits. For that, the Blue pupil center must stay on column 128. This constrain is fulfilled.

Coordinates of pupils center in the current configuration using external sources are [128,198], [62,84], [194,84]. The main difference between optical design and current alignment is a global $9\text{px}=432\mu\text{m}$ shift of the CCD in the vertical direction that has no effect on the performance.

Note also that the Red and Yellow pupil are slightly shifted toward the left side of the CCD: this help in realizing a pupils's geometry closer to the one of an equilateral triangle. In fact, in the FDR geometry the distances between the pupils center are 130, 130.2, 134.1 px, while in the current alignment the distances are 131.7, 131.7, 132 px.

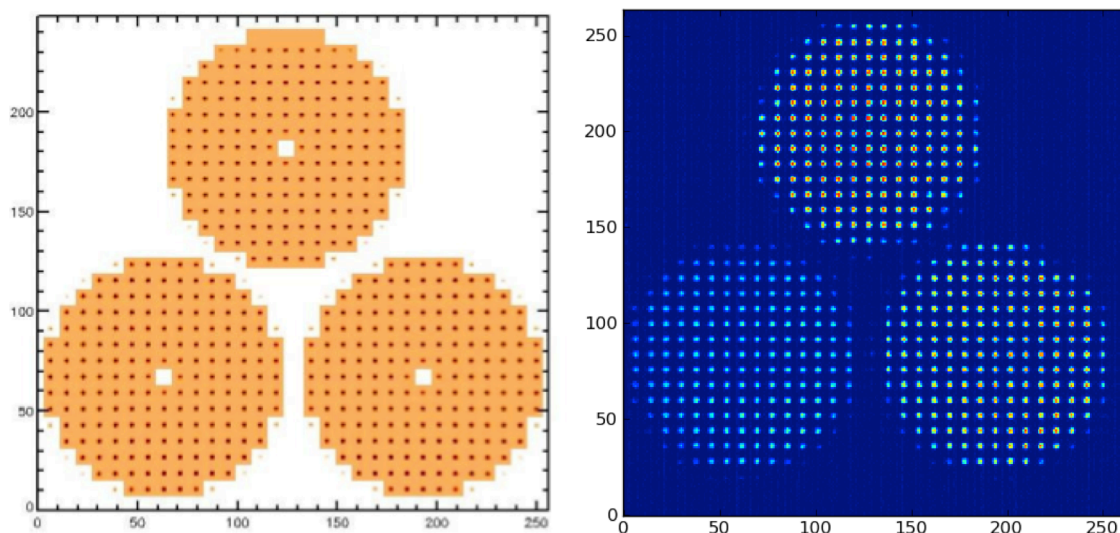


Figure 4 Spot geometry as foreseen at design phase (left, from AD2 Figure 8) and as realized (right, reference 20131214_130800)

6.3 Frame rate

The WFS Camera and BCU slope computation have been successfully tested to a frame rate of 1kHz. Minimum tested and working frame rate is 100Hz. Most of the tests have been done at a frequency of 970Hz (1030us)

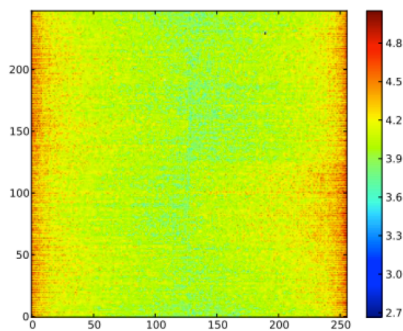
6.4 Read-out Noise

The WFS Camera has been carefully characterized in AD6 and the main parameters have been also measured in an independent way in Arcetri (AD7).

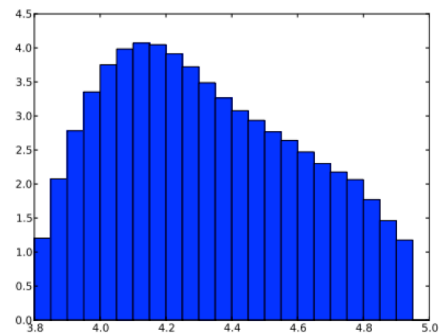
Most of work done in AD6 has been done using the so-called "Optical ADC", a separate device that digitalizes the frame and can feed the BCU frame grabber. Instead the Arcetri camera came with "Microgate ADC", a modified BCU board that allows digitalization of the frame directly on board of the BCU. All the tests on the integrated DX-LGSW have been done using Microgate-ADC.

In a direct comparison done on a different camera unit at MPE the RON using Optical-ADC was found to be 4.3e- and the RON using Microgate ADC was found to be 4.5e-. The slight difference of 0.2e- doesn't motivate the use of the Optical-ADC.

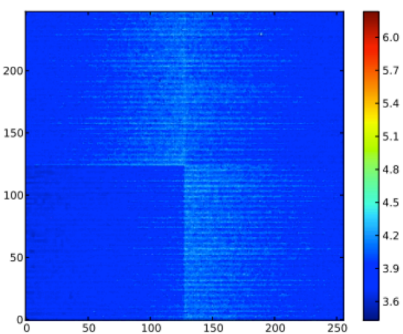
The read-out noise of the camera LBT#2 fully integrated in the DX-LGSW measured in Arcetri is 4.2e- and the gain is 3.9 ADU/e-.



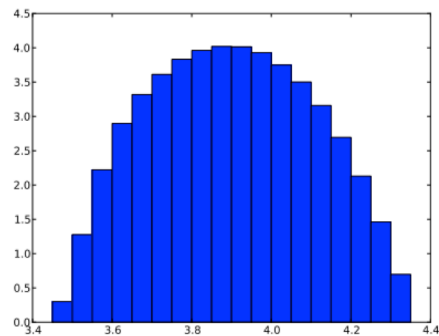
(e) RON map (1 kHz).



(f) Histogram of RON (log scale, 1 kHz).



(a) Gain map (1 kHz).



(b) Histogram of gain (log scale, 1 kHz).

Figure 5 Read out noise and gain map for WFS Camera LBT#2 measured after integration in the LGSW in Arcetri.

6.5 Common Mode Noise residual

The WFS Camera is affected by a common-mode-noise that is visible as rapidly changing vertical stripes in the frames. This chip issue was known since the design phase, and the real-time frame processing on board of the BCU has been designed to mitigate this effect (details in [AD4]).

The residual common mode noise after frame-processing has been studied in detail during camera development [AD6 Sect 3.4] concluding that it is not affecting the global performance of ARGOS.

The noise has been measured also in Arcetri in the fully integrated system.

The effect of the residual common mode is clearly evident in the WFS noise projected on a modal base: the tilt oriented along the CCD rows is affected by a bigger noise than the tip (a plane whose slope is oriented along the CCD column). In Figure 6 we can see that the measurement error on tilt in the high-flux case (1000 ph/subap, 1" FWHM source) is 33nm compared to 10nm on tip.

The same effect affects the jitter stabilization loop, as quantified in Section 13.1 and shown in Figure 10 where the jitter error along CCD rows is about 3 times bigger than the along CCD columns.

6.6 Wavefront sensor measurement error

Refer to Section 25.3 for a complete description about how the wavefront sensor measurement has been assessed. The wavefront sensing error in the high-flux condition (1800 ph/subaps) with 1" FWHM spot size is 42nm rms.

In the design phase [AD3 Sect 7] the wavefront sensing error was required to be 38nm in case of a nominal flux of 1800 ph/subaps.

The final requirement the Top Level Requirement FDR document AD8 was simplified to 50nm.

The closed-loop tests described in Section 25.3 demonstrate that the DX-LGSW wavefront sensing error in this condition is 42nm.

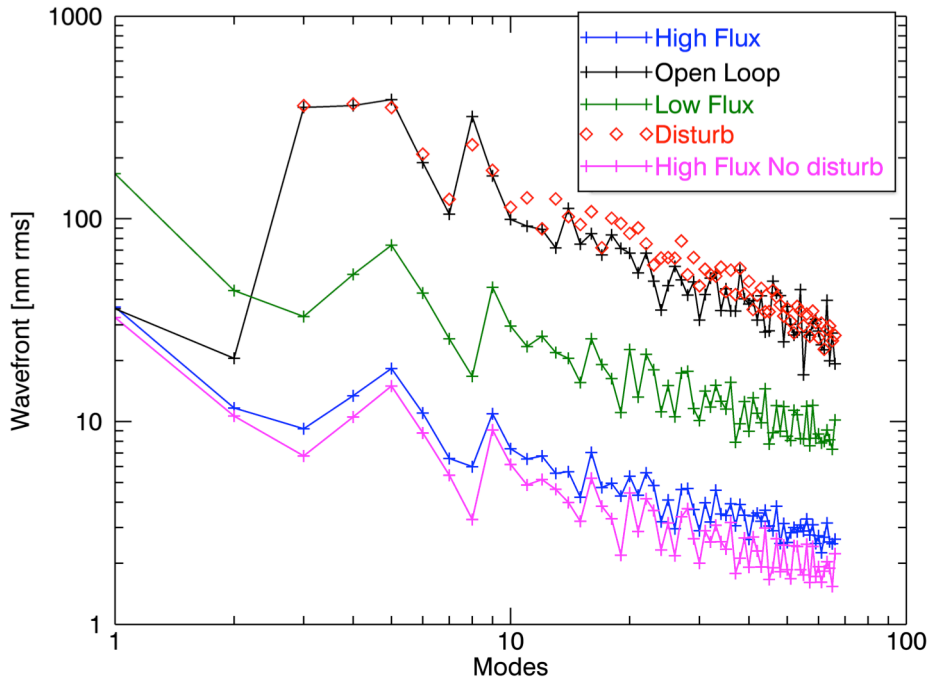


Figure 6 Modal amplitude of residual wavefront before and after correction with the MEMS DM. See Section 25.4 for details.

6.7 Slope computation

The centroid algorithm described in document [AD4] is implemented in the real-time slope computer that runs in the BCU. The algorithm has been checked using a limited set of the parameters' space. In particular the default configuration used for most of the tests in Arcetri is the one called TCoG in [AD4] in its simplest form with threshold=0.

Nevertheless, the software is ready to configure the BCU slope computer using the various options of the centroid algorithm.

As a final note, we have asked Microgate to implement an extension of the algorithm to use the average subaperture flux for the computation of the centroids. This should result in a better noise propagation as experienced with FLAO. This extension to the firmware is still to be implemented and tested.

6.8 Slope RMS

The LGSW must provide to the AARB an indication about wavefront flatness. A meaningful variable could be a 1s-running mean of the slope rms. This parameter is not computed nor exposed to the AARB at the moment.



6.9 Optical transmission

The optical transmission of the WFS has not been measured and it is assessed by design

Element	Surface	Transmission
Dichroic		0.999
Fold mirror		0.95
Entrance window	1	0.995
	2	0.995
Collimating lens	1	0.9975
	2	0.9975
Periscope mirror		0.999
Piezo mirror		0.999
Polarizer I	1	0.99
	2	0.99
BBO I	1	0.99
	2	0.99
RT	1	0.99
	2	0.99
BBO II	1	0.99
	2	0.99
Refocusing lens	1	0.9975
	2	0.9975
Field lens	1	0.9975
	2	0.9975
Collimator I	1	0.9975
	2	0.9975
Collimator II	1	0.9975
	2	0.9975
Lenslet array	1	0.998
	2	0.998
WFS camera window	1	0.9975
	2	0.9975
CCD QE		0.98
Total		0.82

Bottom Line: The LGSW hardware meets all the requirements about wavefront sensing. The WFS camera read-out noise is slightly higher than as by-design, but this doesn't affect the performance. The BCU slope computer algorithm has been verified and extensively tested in the simplest Center-of-Gravity mode that has been proved sufficient for our needs.

7 Gating units

Requirement: LGSW must be capable of range gating the LGS beams. The requirements are defined in the design documents [AD7, AD3 Sect 7.6]: the suppression rate must be >200, laser-to-trigger jitter <9ns and trigger-to-cell-opening jitter <9ns. An additional requirement is about transmittance homogeneity across the pupil: a reasonable estimate is that homogeneity has to be better than 10%.

The trigger is originated by a device in the LALAS system and as such is not part of the LGSW. The trigger-to-cell-opening cannot be easily verified in the integrated LGSW unit.

The gating units suppression rate has been measured after integration in the following way: the opening time T_{ON} has been swepted from 0.1 to $2\mu\text{s}$ and the average flux per subaps per cycle ($100\mu\text{s}$) is stored. The flux ϕ is the sum of 2 contributions: the photons transmitted during close-time (small transmittance ϕ_{OFF} for a long period $T_{OFF}\sim 100\mu\text{s}$) and the ones transmitted during opening-time (high transmittance ϕ_{ON} for a short period T_{ON}). The relation

$$\phi = \phi_{OFF}T_{OFF} + \phi_{ON}T_{ON}$$

is linear in T_{ON} with slope ϕ_{ON} . The intercept at $T_{ON} = 0$ gives the constant term $\phi_{OFF}T_{OFF}$. The suppression rate is ϕ_{ON}/ϕ_{OFF} .

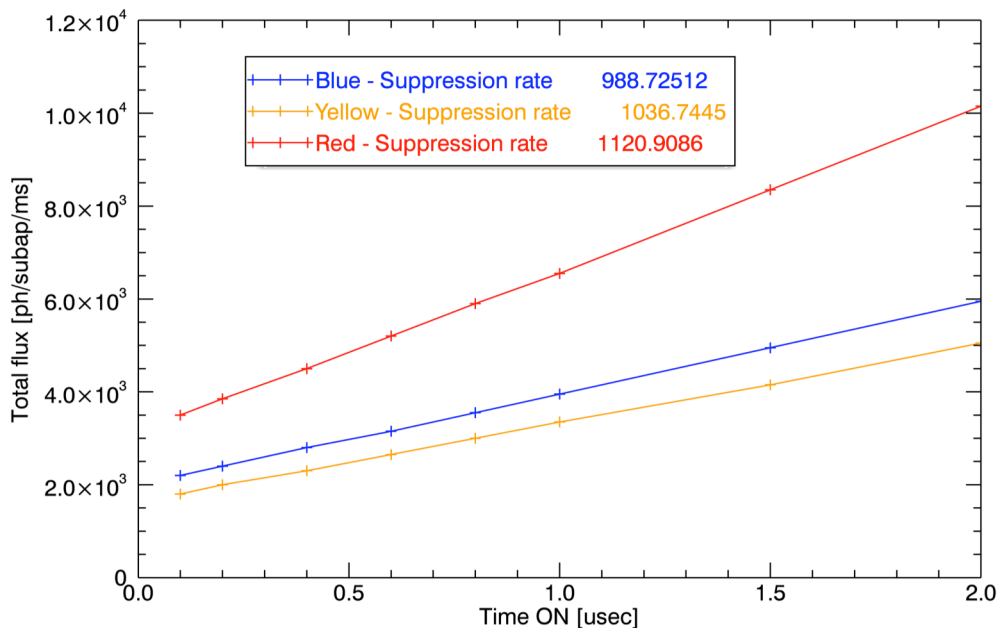


Figure 7 Flux vs duty-cycle of Pockels cells. Close-time T_{OFF} is 100usec

This proves that the suppression rate of the 3 Pockels cell is similar and sufficiently high. The different flux experienced on the 3 pupils is due to the fact that the internal sources exploits the small reflection leak on the high-transmission coating of the entrance windows. The transmittivity of the coating is defined to be >99.7%, meaning that the reflectivity is <0.3%: a small variation in the

coating reflectivity between the 3 windows can easily explain the observed difference in the total flux.

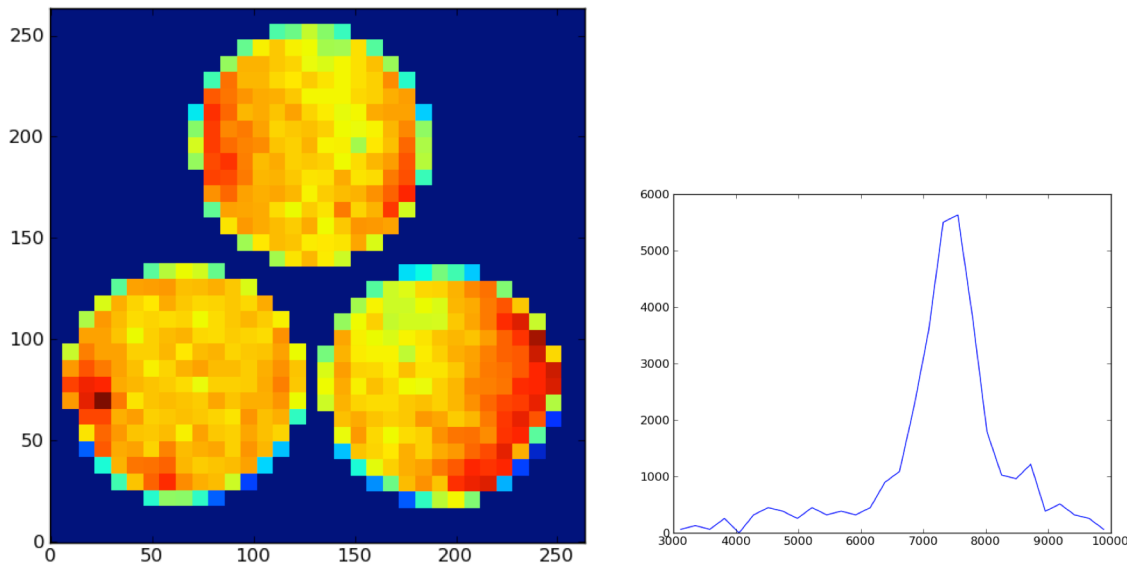


Figure 8 Homogeneity of transmission across the pupils. The histogram on the right shows that the fully-illuminated subapertures have a PtV transmission variation around the median value <20%

The transmission homogeneity across the pupil is shown in Figure 8. Standard deviation computed on the fully-illuminated subapertures is <10% of the median value.

Bottom Line: the gating units are fully functional and fully integrated into the LGSW control SW. The optical and electrical performances meet all the requirements.

8 Sending and receiving slopes

Requirement: LGSW must collect real-time data from the other ARGOS WFSs and send the complete slope vector to the ASM.

The BCU in the LGSW unit is not only computing slopes from LGS beams, but it also collects slopes from the others WFSs, synchronize them and send them to the ASM on the Fast Link optical channel.

Slopes from PyrWFS are received on the Input Optical port. The BCU is still not implementing this feature and a fix is required from Microgate; as well, the control software to configure this feature is still to be implemented **so at the moment the PyrWFS cannot be used as a NGS sensor in ARGOS.**

Tilt signals from Bonn TipTiltUnit are received by the BCU on the serial port and should be asynchronously appended to the LGS slopes (see AD4, Section 5). The communication appears to be correct as tilt signals are actually copied into the BCU memory, but the synchronization with the LGS slopes doesn't work correctly with long stops of up to several seconds. **This issue is impeding to correct tilt using the Bonn TipTiltUnit.**



In all the tests conducted until today by all the groups involved, including Microgate, we never had evidence of a successful stream of slopes signals out of the FastLink channel. Microgate is investigating the cause of this issue. **At the moment, the ARGOS BCU cannot be used for real-time communication with the ASM.**

These issues are of course of paramount importance, but **it is not a stopper for the early commissioning stages.** We expect the fix to require firmware and/or minor hardware upgrades; the 3rd BCU unit is already at Microgate to be used as test-bench.

Bottom Line: The BCU is failing all kind of real-time communications. This impedes to close the AO loop and to acquire AO interaction matrixes. An activity is on going at Microgate to understand and fix these issues.



9 Tip Tilt Unit

Requirement: LGSW must collect real-time data from the other ARGOS WFSs and send the complete slope vector to the ASM.

A minimal functionality test of the Bonn unit installed in the rack has been done. In this test the Bonn unit was configured to send static values (instead of the counts received from the real APD device)

The APD to Bonn unit communication has not been tested in OAA.

The TipTiltUnit has its own dedicate Basdard service that allows accessing and controlling the hardware, **but it is lacking any integration into the LGSW Controller**: it is not configured at boot, it is not started/stopped accordingly to the LGSW State Machine. No work has been done to date to abstract its functionality for its use by a higher layer of software.

Bottom Line: The TipTiltUnit is still not integrated into the LGSW Control software. The brief, basic test done when the unit was first installed in the LGSW rack was positive. But we still need to evaluate its long-term behavior and analyze in details if all the functionalities requested to the unit are available.

10 pnCCD frame grabbing and processing

Requirement: The LGSW Control SW provides the means of acquiring, processing and distributing the pnCCD frames. It also configures the BCU to operate the real-time frame processing needed before slopes are computed.

The pnCCD pixels are collected in the BCU and are processed to subtract dark-frame, correct common-mode noise and apply a pixel gain.

As described in Section 6.4, Optical-ADC have been tested and compared to Microgate-ADC by the MPE team. Optical-ADC was never tested at OAA. To date, the LGSW Control SW assumes that the Microgate-ADC are used. In case we desire to maintain the flexibility of choosing between Optical and Microgate ADCs some modifications in the LGSW Control SW and some characterization of the system are required.

Inputs	Set in the config file	Set at run time	Stored in the calibration tree	Notes
Dark frame	Y	Y	Y	
Flat Frame	N	N	N	Constant=1
Common Mode Map	Y	Y	Y	

A procedure to acquire a dark frame and store it as a FITS file in the configuration folder is commonly used during lab activity.

Bottom Line: pnCCD frame grabbing and processing is fully integrated into the LGSW Control SW.



11 Slope offset

Requirement: The LGSW must be capable of applying an offset to the slope vector. The offset will be modified at about 1Hz from the Truth Sensor loop.

The slope-offset functionality is fully implemented for what concern the BCU configuration. At the moment the slope offset vectors are statically stored in FITS files in the calibration folder. The LGSW Control SW allows to select one of them and to upload it to the BCU.

Inputs	Set in the config file	Set at run time	Stored in the calibration tree	Notes
Slope offset	Y	Y	Y	

In the current implementation a delta-offset measured by the truth sensor must be stored in a file in the calibration folder before being applied. **This is very inconvenient for the truth-sensor-loop running at about 1Hz.** A different SW approach is required for delta-offset received from the Truth sensor and is still to be implemented. Developing this feature doesn't require any HW availability.

A procedure to acquire the slope offset vector and store it as a FITS file in the configuration folder is commonly used during lab activity.

Bottom Line: Slope offset is integrated in the LGSW Control SW, but is lacking the capability of being modified at run-time by the Truth Sensor.

12 Pupil Stabilization

Requirement: The LGSW must stabilize the 3 LGS pupils on the lenslet array within 0.1 subaperture with respect to the position they had when the interaction matrix was acquired.

The pupil stabilization loop stabilizes the 3 pupil images on the lenslet array to compensate for flexures and misalignments. An algorithm based on Sobel edge-detection and Hough transform is used to determine the position of the pupil onto the lenslet array. A proportional gain 2x2 matrix (a.k.a. Reconstructor) converts the position error into the motor offsets.

The goal of the control loop is to maintain the position of each pupil within 0.1 subapertures from its target position.

Motors are moved only when the error is above a given threshold to avoid unnecessary use of the mechanics.

Accuracy is measured as the positioning error for the 3 pupils along x and y (in the reference system of the pnCCD) expressed in subapertures units.

The algorithm to estimate the position has been tuned to add robustness to the system: the position measure is the median value of several independent measurements and there is a quality indicator that is used to flag each measurement as valid. We have proved this algorithm to be robust against sudden loss of light and against frames with artifact. It is not robust when the pnCCD exhibits the “stripes” behavior.

The “capture range” of the loop is greater than 5 subapertures.

Typical measurement accuracy in the high flux regime (1000 e-/subaps/frame) is about 0.02 subap rms.

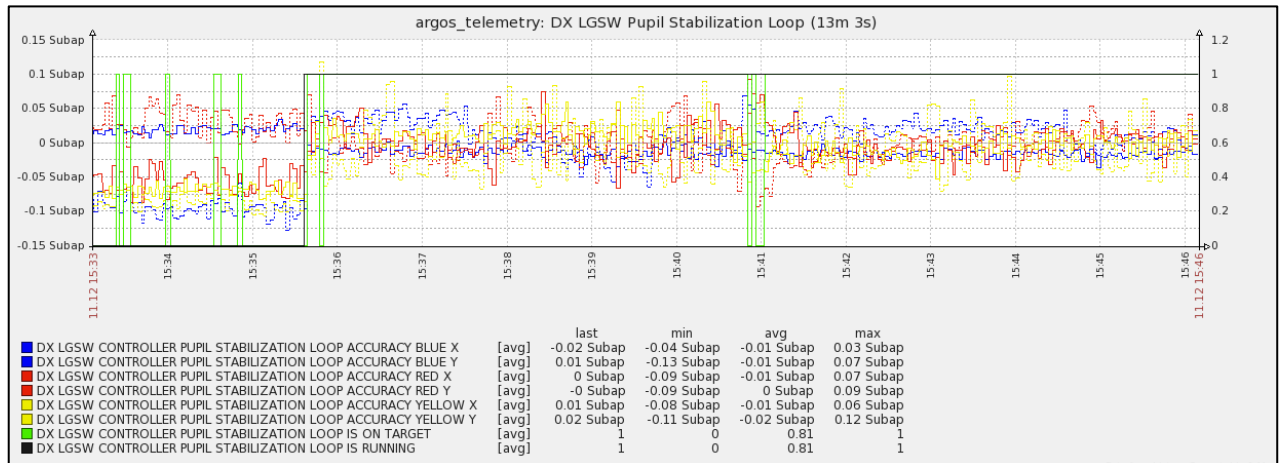


Figure 9 Pupil stabilization loop accuracy in absence of external perturbation.

Inputs	Set in the config file	Set at run time	Stored in the calibration tree	Notes
Reconstructor	Y	Y	Y	
Target position	Y	Y	Y	



DX-LGSW integration report

Doc: ARGOS Tech Note 120

Issue 2

Date 30/01/2014

Page 21 of 50

Gain	N	N	N	It is a constant in the code
------	---	---	---	------------------------------

Outputs	Accessible by SW	Saved in telemetry	Saved in snapshot	Notes
Accuracy	Y	Y	Y	Always available when frame grabbing is possible
isOnTarget	Y	Y	Y	All the 3 pupil are within 0.1 subapertures from target
Pupil optical magnification	N	N	N	The pupil optical magnification (pupil diameter in lenslet unit) is not measured

On 1 occasion in several tens of hours of operation we have observed an effect similar to motor “loss-of-steps”: the steps count slowly drifted to the software limit without an actual correspondent movement of the stage. It looks like the loop required offsetting the stage by such a tiny amount that the motion was then nulled by some mechanical backlash. Re-homing and re-setting to initial position brings the stage back to the nominal position.

Bottom Line: The pupil stabilization is fully implemented and integrated into the LGSW control software. The loop has been thoroughly tested in lab conditions proving robustness and accuracy. We have an indication that there may be a “loss-of-steps” effect that requires re-homing the motors.

13 Jitter Stabilization

Requirement: The jitter stabilization loop compensates for residual atmospheric tilt in the LGS beams to let the LGSW working in the favorable zero-tilt condition.

The residual tilt is estimated by the BCU as the average value of the slopes (along X and Y) for each of the 3 LGS beams. This 6-element vector is copied to the BCU HVC boards that control the PI334.1SL piezo heads. A pure integrator control scheme is implemented in the HVC code to send commands to the piezo heads. For each LGS beam the algorithm requires a proportional gain 2x2 matrix (a.k.a. Reconstructor) and an initial position 2-elements vector to set the.

The scheme does **not** provide a signal-offset capability to set the working point away from 0.

The loop gain must be included in the reconstructor matrix, which can be changed at run time.

The initial position vector is required because of the non-monotonic nature of the tilt-measurement: a large initial piezo command could steer the spots in the adjacent subaperture resulting in a wrong slope command that will make the loop converging around the wrong tilt value. The initial position vector is measured during the LGSW internal alignment and it has been found to be stable during all the lab tests.

Inputs	Set in the config file	Set at run time	Stored in the calibration tree	Notes
Reconstructor	Y	N	Y	
Initial position	Y	N	Y	
Gain	N	N	N	A constant in the code

Outputs	Accessible by SW	Saved in telemetry	Saved in snapshot	Notes
Residual stdev	Y	Y	Y	Computed in both open and closed loop
Mirror Commands	Y	Y	Y	
isLoopRunning	Y	Y	Y	

13.1 Tilt estimate accuracy

Jitter stabilization loop performance in absence of external perturbation is shown in Figure 10. For the first 3 minutes of acquisition the loop was open, so the tilt stdev was mainly due to noise in tilt estimate, which in turn is related to the WFS camera noise. Noise along X direction is clearly higher than in the Y direction because of common-mode correction residual. After closing the loop at 15:55 the noise doesn't increase, as expected from a stable loop. At 15:58 the flux is reduced to about 875 ph/subap/ms. At 15:59 it is reduced to 625 ph/subap/ms. At 15:41 the flux is increased to the original value of 1750 ph/subap/ms.

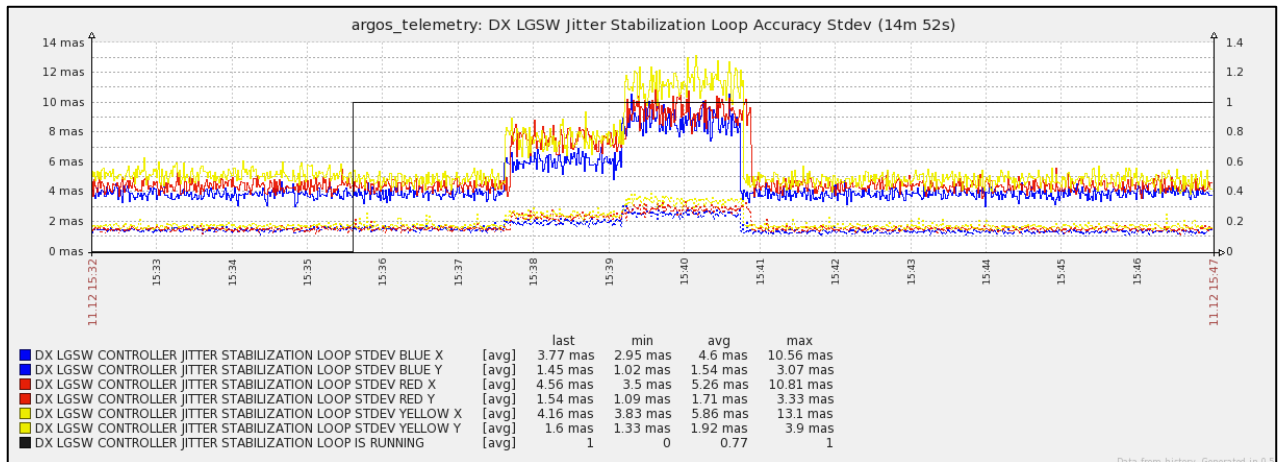


Figure 10 Jitter stabilization loop performance in absence of external perturbation. On Y-axis are reported the tilt standard deviation on the 3 pupils (blue, yellow and red) along X (solid) and Y (dashed). Units are tilt angle on-sky. Each point is the standard deviation of a set of 100 tilt values computed by the BCU as the average over each pupil of the slopes measurement. It is converted to on-sky angle assuming a WFS FoV of 4.5".

13.2 Piezo Mirror Commands

The commanded positions of the piezo mirrors are logged in the telemetry and are accessible from the SW interface. We have observed some coupling with the pupil recentering: when the pupil motors are moved, a tilt is introduced that is rapidly compensated by the jitter stabilization loop. This effect is present from the design and is not affecting the jitter stabilization loop performances because of the fast response of the latter compared to the pupil motors.

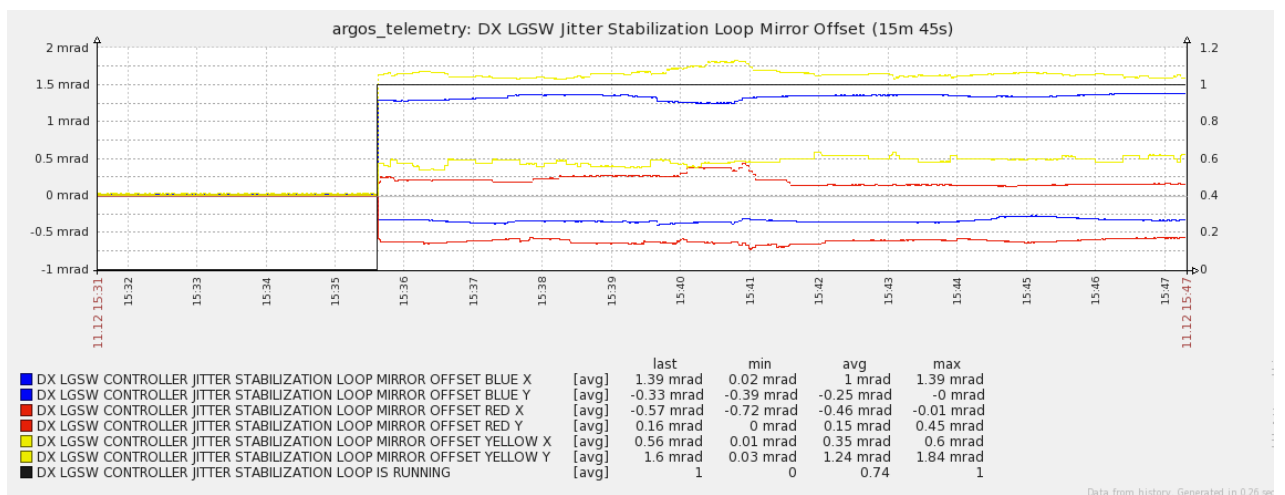


Figure 11 Command to piezo mirrors. Same time range of Figure 10. To null the tilt only a small fraction of the full range (+/- 15mrad) is used. In closed loop we observe slow oscillations in the order of 0.1mrad (probably a CCD thermal effect) and sudden steps that are due to some coupling of the tilt with a shift the pupil motors.



13.3 Dynamical performances

The closed loop transfer function of the jitter stabilization loop is still to be measured. **An automatic gain-estimation procedure will be needed to fine-tune the gain value at the telescope.**

Bottom Line: The jitter stabilization is implemented and integrated into the LGSW control software. The loop has been tested in lab conditions proving robustness and accuracy. Dynamical performances are still to be optimized and quantified. SW scripts to optimize performances are still to be developed.

14 LGS spot size estimation algorithm

Requirement: LGSW must provide an estimate of the size of the LGS spots averaged on a long period. This estimate is used by AARB as input in a control loop that focuses the LGS beams by adjusting the launch.

Bottom Line: The LGS spot size measurement is not yet implemented in the LGSW Control SW.

15 Wavefront focus estimation algorithm

Requirement: LGSW must provide an estimate of the wavefront focus of the 3 LGS beams averaged on a long period. This estimate is used by AARB as input in a control loop that offloads the LGS focus by adjusting the Pockels cells' delay.

Bottom Line: The focus estimate is not yet implemented in the LGSW Control SW.

16 Acquisition cameras

Requirement: LGSW must patrol a field of 60" to detect the LGS beams and provide their position to the AARB for the laser acquisition step.

The 3 patrol cameras are fully integrated in the DX-LGSW and are fully functional. The low-level software is the same used for the cameras in the LALAS system. The acquisition algorithm to estimate the position of the LGS beams has not been implemented yet.

The field of view of the patrol camera for the Blue arm is 66x55".

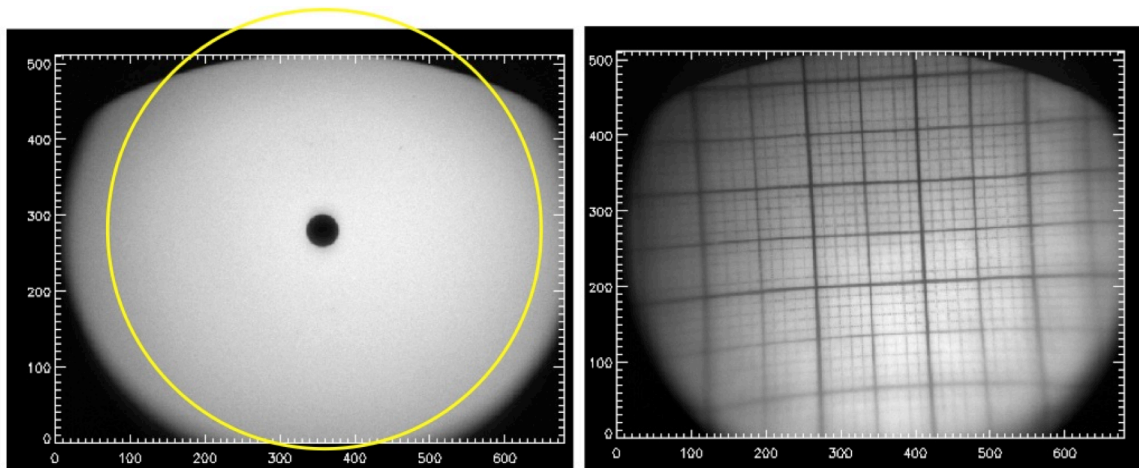


Figure 12 Patrol camera FoV for the Blue beam. Yellow circle outline a 60" circular field. The actual field is elliptical with axes 65 and 55". Pixel scale at binning 2 is 0.1"/px

Bottom Line: The patrol cameras are integrated in the LGSW and are fully functional. The algorithm to determine the position of the beams is still to be implemented. The software interfaces to expose beam positions are missing in the LGSW Control SW.

17 Cooling and dry air circuits

The cooling circuit is made of 2 independent circuits. One operates with water at 6°C constant temperature and is used for the WFSCamera. The second one feeds "regulated" water following the greater among ambient temperature and 6°C.

The regulated water is used to cool (or to warm, when ambient temperature is below 6°C) the patrol cameras and the Pockels cells driver.

18 Internal sources and external sources

Requirement: LGSW must provide an internal source to check internal alignment and devices functionality. The internal source needs to provide a flux comparable with the expected flux from the LGS.

A DiodeSource module custom made at MPE is embedded in the IOSwitch module. At the telescope it will feed the internal calibration unit that can be used to check the functionality and raw-alignment of the LGSW.

It is important to note that the LED source is not polarized, nor narrow-band as the laser beams from sky. As a consequence we may expect a slightly different behavior of the LGSW when on-sky in terms of transmission.

The internal source exploits a reflection on the entrance window that is coated for optimal transmission at 532nm. This means that the flux is quite low. At maximum power (0.7A in the diode) the flux is about 4000 ph/subap/ms. At minimum power (0.03A) is about 300 ph/subap/ms.

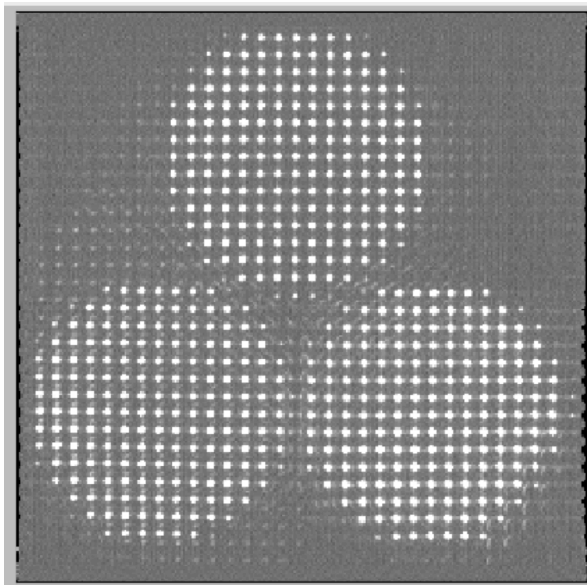


Figure 13 Ghosts when using internal source.
 Color scale exaggerated to see details.

Some ghosts spots are visible in the CCD image when using the internal source: this was expected from the design phase and it is due to the multiple reflections on the LGSW entrance window that is coated for high transmittance. This effect is not compromising at all the functionality and the use of the internal source.

During the lab tests the same DiodeSource has been used to feed 3 temporary external sources producing an f16.6 beam focused on the entrance windows of the LGSW. Each external source produces 2 spots, one on-axis centered into the LGSW FoV and one about 10" off-axis visible from the patrol cameras. The images produced on the patrol cameras are NOT equivalent to the ones expected from the sky, the latter being affected by Rayleigh scattering from all the atmospheric layers, probably producing a halo around the spot.

The external sources cannot be left installed at the telescope because they obviously interfere with the beams from the telescope.

The diode source module had an issue during the cold test (see section 24.1.3) that requires to be clarified.

Bottom Line: The internal sources are tested and integrated in the LGSW Control SW. The delivered flux is ok. Some ghosts are visible as expected from the design of the unit.

19 Storing and management of calibration

We distinguish between *configurations* and *calibrations*.

Configurations files are used to define the behavior of the various pieces of hardware and software that form the LGSW. They are saved in the svn tree together with the ARGOS code.

A calibrations file is obtained via a measurement of some system's property and it is subject to change with time. Typical examples are the dark frames of the WFSCamera, the slope-offset vector, the interaction matrix of a control loop.

The following properties are currently *calibrations* in the LGSW:

- Common Mode Map
- Dark frame
- Flat frame
- Jitter Stabilizer Initial Position
- Jitter Stabilizer Reconstructor
- Pupil Stabilizer Target Position
- Pupil Stabilizer Reconstructor
- Slope Offset
- Subaperture Definition

Calibrations files are quite big and their number grows with time so it was decided not to store them in the svn repository. They are saved in the disk of the DX-LGSW workstation. The LGSW SW uses "tags" to identify the calibration and retrieve it. Great care has been used in the SW to keep track of the tags in the telemetry in such a way that a off-line analysis can completely reconstruct the configuration of the system.

20 Diagnostic and telemetry

20.1 Real-time data from LGSW BCU

Real-time data can be collected from the BCU via the diagnostic channel streaming on the Ethernet link. The data available in the diagnostic record (described in detail in the Microgate documentation [XX]) consists of CCD frames, slope vector, jitter and jitter stabilization commands, TipTiltUnit counts and slopes, ASM modes, commands and position when available.

The SW module that is devoted to collect the diagnostic stream from the BCU is able to acquire slopes records at full rate (1kHz, no loss on 10 acquired set of 4000 records) together with CCD frames at 40Hz (no lost frames on 10 set of 160 frames). To be on a safe side, the BCU is typically configured to stream CCD frames at 25Hz.

In a single operation a client of the diagnostic collector can retrieve up to 4000 diagnostic frames a) from a circular buffer containing the past ones, or b) waiting for the future ones.

The off-line download of the full memory buffer from the BCU (containing up to 700? consecutive CCD frames) is technically possible but it is not implemented in the LGSW Control SW.



REFERENCE: speed test in sandbox.measureBCUDiagnosticBasdardSpeed

20.2 Snapshot

The LGSW control software allows grabbing a full snapshot of the LGSW system and storing it on disk. The snapshot typically consists of 4000 real-time diagnostic slope frames, a few tens of pnCCD frames and some patrol cameras frames stored in several FITS files.

```
[argos@dx-lgsw ~]$ ls snapshots/measures/DX/20131217/20131217_183259/  
apd_counters.fits  
asm_dist_average.fits  
asm_ffcommands.fits  
asm_integrated_modes.fits  
gain.fits  
info.fits  
jitter.fits  
jitter_piezo_commands.fits  
jitter_piezo_positions.fits  
lgsw_ccdframes.fits  
patrol_camera_blue.fits  
patrol_camera_red.fits  
patrol_camera_yellow.fits  
slopes.fits  
slopes_frame_counters.fits
```

The header of each FITS file contains a global snapshot of the system; at the moment of writing the header has 251 keys containing hardware status, calibrations in use, quality indicators for internal loops, software main parameters, etc.

At the time of writing the snapshot feature is implemented for the LGSW only and it is not in its final configuration. LALAS system and AARB may in the future implement a similar mechanism to save their data in the snapshot.

Snapshots stored on disk can be analyzed using a version of the “elab_lib” developed for the FLAO system that is being specialized for ARGOS. **The ARGOS elab_lib is at the moment only marginally implemented.**

20.3 Telemetry and monitoring

The LGSW Control SW makes use of the ZABBIX monitoring system to keep a history of the most important parameters.

ZABBIX keeps the full history for about 3 months and decimates the older records.

ZABBIX allows defining triggers to react when certain conditions are met (for instance by sending email with the description of the event)

At the moment of writing 94 DX-LGSW variables are logged. List includes:

- LGSW Controller status (state machine, loops On/Off)
- Devices reachability

- WFS Camera status (Water and CCD temperature, PEC current)
- Motor position
- Pupil stabilization loop parameters
- Jitter compensation loop parameters
- Temperature and Humidity readings
- Average Flux per subap.

This tool is extremely useful for debugging: we plan to add more variables in the future.

The following triggers have been defined in ZABBIX:

- Temperature in the Patrol Camera water circuit exceeding the temperature of the main circuit by $>2^{\circ}\text{C}$ on a 5min time-scale
- Temperature in the Pockels Cell Driver water circuit exceeding the temperature of the main circuit by $>2^{\circ}\text{C}$ on a 5min time-scale
- Temperature in the WFSCamera water circuit $>18^{\circ}\text{C}$ when Peltier is on
- WFSCamera pressure $>55\text{mbar}$
- WFS Rack temperature $>25^{\circ}\text{C}$
- Pockels Cells driver is in fault

When one of these conditions is met ZABBIX sends an email to a configurable mailing-list, describing the event. An OK email is sent also when the error is no more detected.

This functionality is on top of the automatic safety reactions and can help the operator to quickly identify the arising of pathological conditions.

Bottom Line: The building blocks and basic framework for diagnostic tools for the LGSW are implemented and tested, with positive results in terms of performances. The full integration of all the important variables in the snapshot and in the ZABBIX telemetry is still to be completed. The off-line analysis tool is not implemented.

21 Safety

The following active and passive safety features are implemented in the LGSW:

1. WFSCamera: if the water temperature is too high the camera shuts down and warms up.
2. WFSCamera: if the pressure or humidity values inside the camera are outside the acceptable range the camera shuts down and warms up.
3. Electronic rack: the rack has a hardware circuit to cut the power in case of temperature too high.
4. Cooling water temperature: when it exceeds absolute thresholds (-5°C and 30°C) the LGSW Control SW triggers a so-called *housekeeping error* that fires a delayed shutdown and power off of the LGSW system.
5. Ambient and rack temperature: when it exceeds absolute thresholds (-25°C and 35°C) the LGSW Control SW triggers a *housekeeping error* that fires a delayed shutdown and power off of the LGSW system.
6. SW basdards: if a server crashes the LGSW Controller goes in an error state.
7. Device errors: in case a device is not reachable from its server the system goes in an error state.

There isn't any kind of protection against a malfunctioning of the cooling circuit: if the water temperature is too low or too high the system has no way to protect itself.



Housekeeping error triggered by the THOR devices has been checked during the cold test. The manifold regulator was badly regulated and the coolant flux into the patrol cameras was so small that the ambient air-cooled the cameras to a point below the operating temperature of the cameras (-5C). In this condition a housekeeping error was fired and after a timeout of 500s the system was shut down and powered off (REFERENCE 20131218_152200).

Bottom Line: A framework to react to ambient hazards and errors condition has been implemented in the LGSW. Individual devices and system software are programmed to shutdown and poweroff in case of hazards. It is important to note that the system



22 Maintenance

22.1 Twiki

A public twiki details the list of HW devices used in the LGSW systems. It is accessible at <http://aowiki.arcetri.astro.it/ARGOSPublic/WebHome> and it has been created to collect all the relevant information for the maintenance of the system. LBTO and ARGOS technicians are supposed to access this twiki for all maintenance operations and contribute with discipline to keep track of every HW failure, HW configuration and build a history for every device in the LGSW. It will also collect documents about handling and installation of the LGSW.

22.2 Spare parts

Spare parts are available. The full list is given in Section 27

22.3 Proprietary software tools

Many of the devices come with some proprietary software tools (typically running under Windows OS) to configure and operate the device during maintenance. These tools have been collected on a Windows Virtual Machine running on the DX-LGSW workstation. This will ease the maintenance in the case of basic tasks like discovery or changing the IP address of a new device, upload a new firmware, etc.

Bottom Line: Some tools have been put in place and are commonly used by LGSW engineers to facilitate the maintenance of the system and create a documented history of the LGSW components. Most of the needed spare parts are available.

23 Appendix A - Gravity test

The LGSW unit is mounted on a tiltable bench. The system is maintained in open-loop to measure deflection of pupil position (measured by the pupil stabilization loop) and pointing offset (the slope tip-tilt measured by the jitter stabilization routine). The full 0-90° elevation range is spanned.

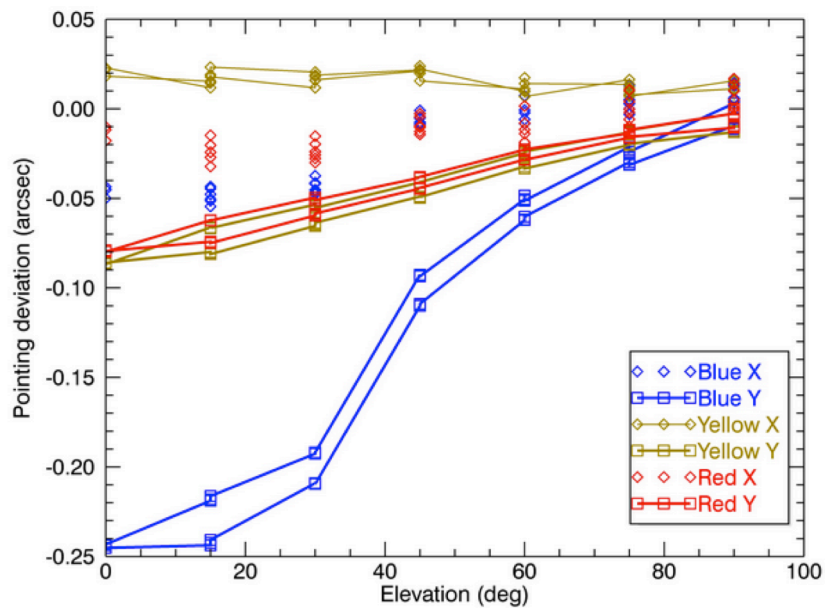


Figure 14 Pointing deviation during a complete 90-0-90° elevation test. Solid lines correspond to deviation along the Y axis.

Figure 10 shows the pointing offset during the elevation test. As expected from the geometry of the flanges supporting the optics, the mechanical flexures are more evident along the Y axis, in particular for the Blue beam that is the one more distant from the optical breadboard on which the flanges are screwed. The offset along the X-axis are negligible and within the measurement error. The hysteresis is negligible as well. The maximum pointing deviation in the full operative elevation range (90-30°) is 200mas and it is compensated by the jitter compensation loop using a small fraction <10% of the piezo heads stroke.

The pupil stability during the elevation tests is shown in Figure 15. The pupils moved less the 0.2 subaperture that is a tiny fraction of the full range of the pupil stabilization loop.

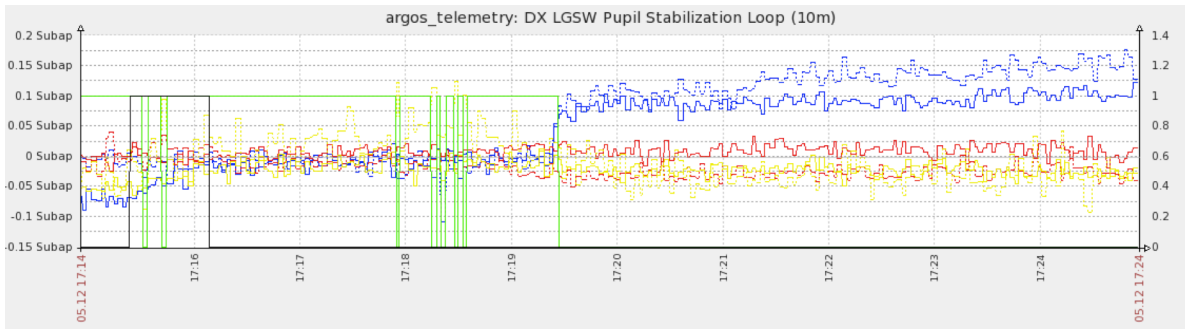


Figure 15 Pupil stability during a 0-90° elevation test. Pupil offset is <0.2 subaps, a tiny fraction of the pupil stabilization loop range

24 Appendix B - Thermal Cycling

A test of the unit in a cold environment has been performed to assess the system's functionality and performance at low temperature.

The test has been performed from 6th Dec 2013 to 19th Dec 2013. The system has been moved into a refrigerated truck at Arcetri's lab and 5 thermal cycles have been performed changing the LGSW tilt angle from 0° (zenith pointing) to 90° (horizon pointing) and using both internal and external sources.

During the whole test the system has been fed with coolant at temperature 7-10°C using an external chiller. The LGSW has been kept on and in operating state ("ALL_LASER_ACQUIRED" with pupil and jitter stabilization loops active) most of time, frequently acquiring snapshots of the system.

A typical sequence of acquisition consists in:

1. Shutting down the system, without powering off the rack and without stopping the chiller.
2. Wait a few minutes to let the external devices thermalize at ambient temperature
3. Power on and setup the system
4. Acquire a dark frame and apply it
5. Acquire a set of slope offset and apply it
6. Acquire 3 snapshots of 8 seconds of real time data and patrol cameras images.
7. Acquire 1 snapshot of 100 pnCCD frames at dark to analyze RON.

This sequence proves the functionality of the devices during boot and during shutdown and allows collecting information about the dependence on temperature of the optomechanical stability of the system.

The above-described sequence has been sometimes modified to allow for a fully cold start of the system. In this case the rack has been fully powered off. In all the case the cooling circuit has been kept on.

We need to stress here that a "storage-test" of the devices (no power, no coolant, thermalized to cold ambient temperature) is not part of this test and we remind that the system (electronic rack, cameras, Pockels cell driver) is actually "warmed" by the 6C coolant in case of cold external temperature. Here we intended to test the functionality of system under operative conditions, i.e. after having being connected to cooling circuit and thermalized.

REFERENCES:

- <http://aowiki.arcetri.astro.it/ARGOS/Diary20131206>
- WFSCamera failure (?) in the cold - email thread 14/12/2013

24.1 Devices functionality at low temperature

The following anomalies were detected:

1. WFSCamera failure during Power On
2. Internal THOR failure at boot
3. DiodeSource faints at high diode current at low temperature (current overload)
4. THOR reading glitches (2 times)

5. WFSCamera stripes (repeatedly, apparently not related to cold environment)
6. WFSCamera PEC glitch (occasionally, apparently not related to cold environment)
7. DeviceUnreachable (sporadic on Patrol Cameras and Pulse Generator, SW fixed)

24.1.1 WFSCamera failure during Power On

When started at very cold temperature the WFSCamera fails during powering on of the CCD. From the kontron-pc logs it seems that the CCD is powered on but powered off soon after. The reason is identified in a current value of the power supply that is outside of an allowed range. The workaround implemented by GOX consisted in enlarging the allowed range:

+BUFFER and -BUFFER currents limits were at min. 220mA, and are now at min. 200mA.

After this software fix, the WFSCamera was able to power on at -20C.

We stress the fact that a similar fine-tuning of software limits can be required again in the future.

WHEN: repeatedly when air temperature is about -20C (20131214_150000 till 20131216_110000)

24.1.2 Internal THOR failure at boot

The THORs are powered by a 5V power supply that is hosted in the MOCON module. The power supply can be enabled/disabled by a remote switch controlled by a webI/O hosted in the Dichroic and IOSwitch module.

The failure has been observed 4-5 times below -10C, with LGSW electronic completely switched off and system thermalized. When the system is powered-on the internal THOR remains unreachable, doesn't accept any connection and doesn't reply to a ping.

Trying to power-cycle it using the webI/O always fixed the problem. This could be related to an issue in the THOR itself, in the power supply or in the webI/O. THORs were already tested standalone in the freezer with success. In that case, THOR was powered by an external tunable power supply. We already noticed on the patrol cameras that at very cold temperatures the Ethernet module could require a higher-than-average voltage to boot. A possible workaround is to increase the voltage of the 5V power supply.

For completeness, the External THOR was powered by an external USB powered supply during the test, so it was never switched off and didn't show any problem, but it could be affected as well by this same issue.

24.1.3 DiodeSource faints at high diode currents

In the first thermal cycle the electronic rack was badly isolated and the internal temperature went down to a minimum of -6C instead of the operation temperature of +6C.

In this abnormal condition the diodesource suffered of shutdowns when high diode currents were required (error -310, current overload). After a better insulation, temperature inside the electronic rack was always above 0C but this effect was observed a couple of time more (e.g. on 20131218_142500).

This effect was never observed in the lab where a similar device was extensively used with an external power supply. At the moment of writing the experience with the DiodeSource installed in the IOSwitch module is very limited.

24.1.4 THOR reading glitches

In 2 different occasions the system recorded a glitch in the reading of some sensors from THORs devices. This was never observed at room temperature. The software reacted with a Housekeeper Error; to make it more robust to glitches it could implement a median filtering.

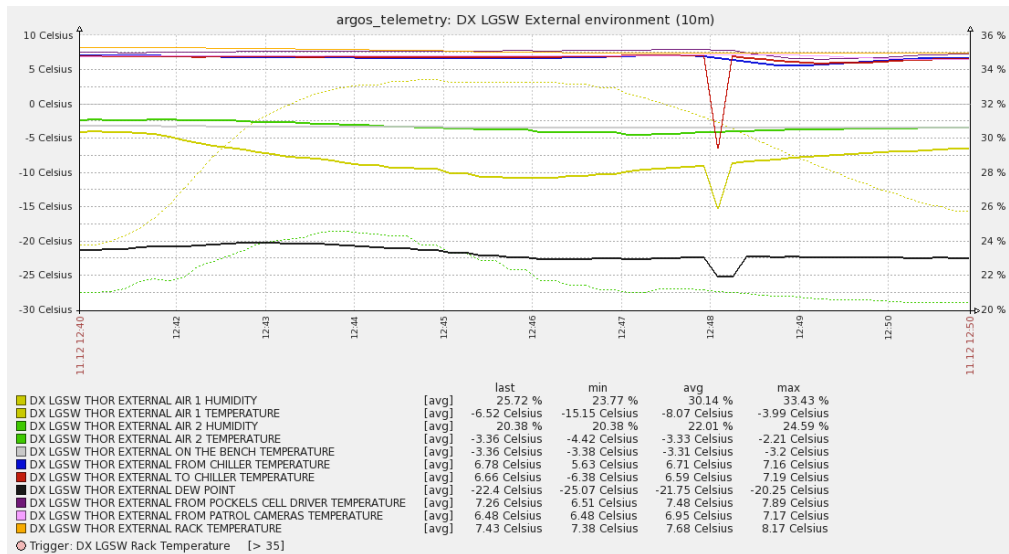


Figure 16 Glitch in the reading of environment monitor THOR.

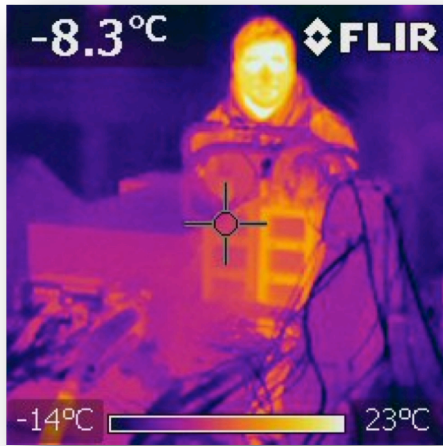
Bottom Line: During the cold test the functionality of the LGSW devices was quite good. We don't report any failure related to the optomechanics devices. We report issues with THORs and Diode Source that we suppose to be related to some electrical/power-supply settings.

UPDATE 2014-01-10: Due to a failure, we removed the WFSCamera LBT#1 used during the cold test and we installed the WFSCamera LBT#2, previously installed in the SX unit. As a consequence, the WFSCamera LBT#2 now installed in the DX unit has not gone through the cold test after full integration of the system. A standalone cold-test of the head has been done in MPE.

24.2 Optomechanical stability of Wavefront Sensor during thermal cycles

Compute slope variation during the test at zenith and horizon etc.

24.3 Thermocamera measurements



Thanks to the very low winter temperature in Florence at the moment of the cold test we were able to open and enter the refrigerated room without causing condensation and we could get some pictures of the running LGSW with a thermocamera.

The freezer set point was -10C, air temperature was in the range -10C/-5C and the LGSW was slowly cooling down. At the moment of the measurements the table temperature was about -8C and the air inside the LGSW was about -4C. Coolant was circulating at 6C. Temperature inside the rack was 18C. We believe the precision of temperature estimate from thermocamera pictures during our test is about 1-2C; the precision has been estimated by

measuring several times the temperature of the same component from different directions. Uncertainty appears to be related mostly to the unknown emissivity of the surfaces, that we assumed to be constantly 0.95.

The thermophotos show that there are 2 delicate parts of LGSW that deserve particular attention to fulfill the thermal requirements: the Pockels Cells Driver and the Patrol Cameras. The Pockels Cells Driver is adjacent to the exterior of the LGSW enclosure and hosts the high-voltage, high-frequency electronics that drive the Pockels Cells crystals. It is a bulky (about 10kg) metal box liquid-cooled at 6C. The infrared measurement is about 7C. **The Pockels Cells Driver requires to be thermally insulated.**

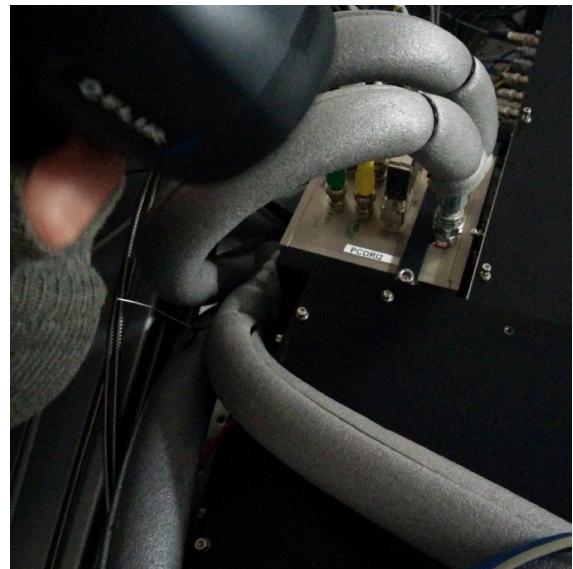
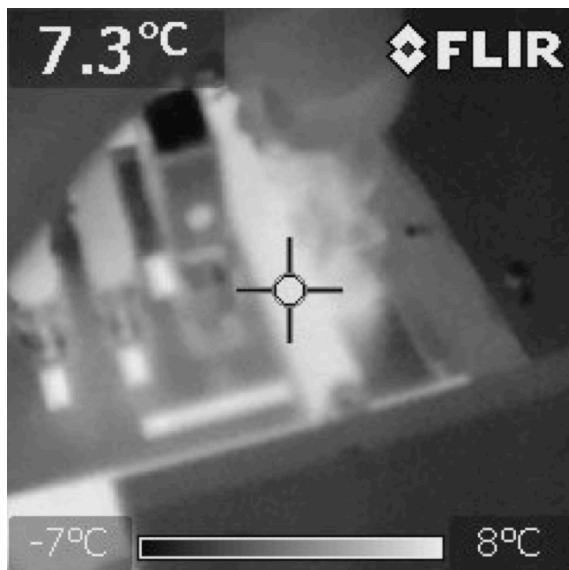


Figure 17 Pockels Cells Driver enclosure temperature is about 7°C. It has been measured on the black-anodized support assuming emissivity 0.95.

The Patrol Cameras dissipate about 5W maximum each and are cooled (actually warmed) at 6C via GPU cooling blocks. The measured temperature of the external housing is about 2C. **The Patrol Cameras must be thermally insulated.**

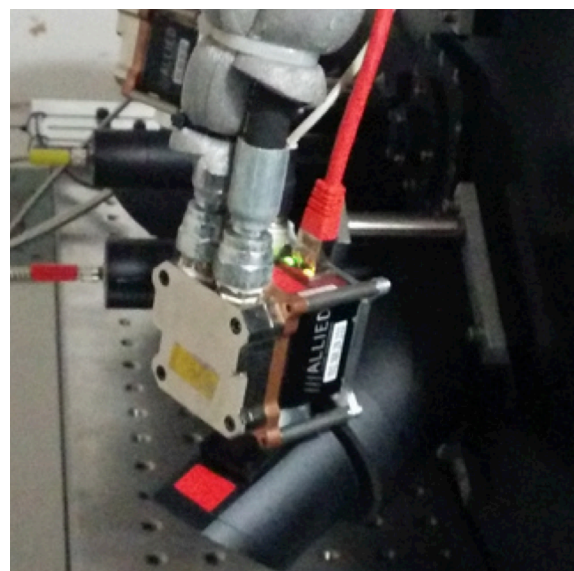
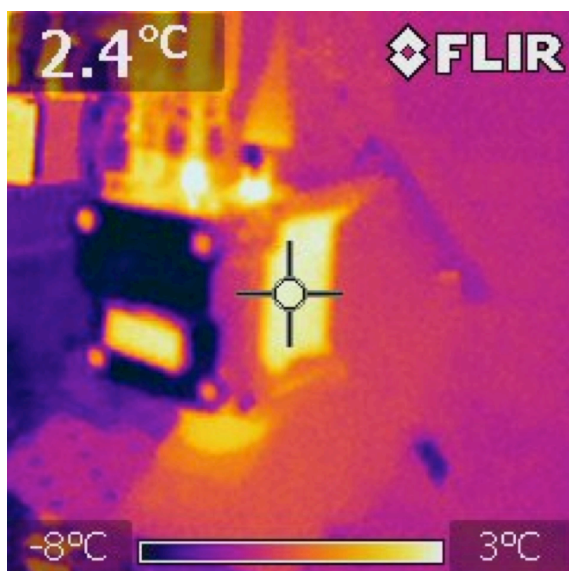


Figure 18 Patrol Cameras temperature is about 2-3C. The heat exchanger block is also at about the coolant temperature but appears cold because of its polishing that reduces emissivity and reflects radiation from the freezer walls.

WFS Camera thermal behavior is very good: the housing surface temperature was -5C, exactly the same temperature of the LGSW enclosure at the moment of the test.



Figure 19 WFS Camera housing is well insulated: the housing surface temperature is -5C, the same temperature of the LGSW enclosure. The measurement has been acquired on the white label that is the only area of the camera surface presenting high emissivity.

The External THOR is also OK: its temperature was -7C, has in the surrounding area.

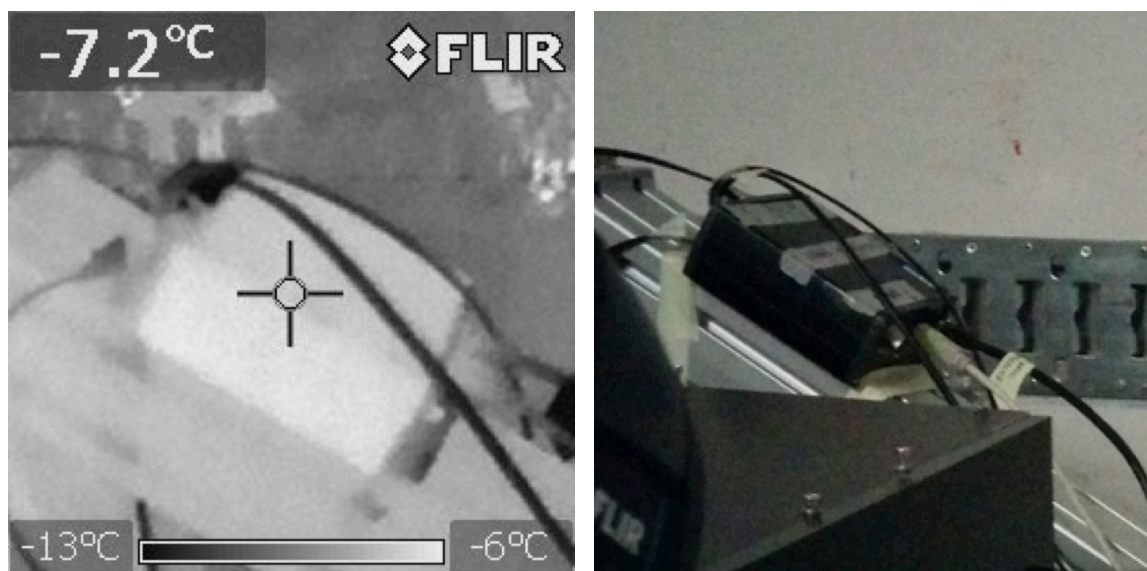


Figure 20 The external THOR during the cold test has been fixed to the tilt table. The temperature of the enclosure is -7C, very close to the one of the surrounding area.

The foam selected to insulate the cooling pipes appears to be effective, as shown in Figure 21. The entire length of the pipes will be covered with insulating foam.

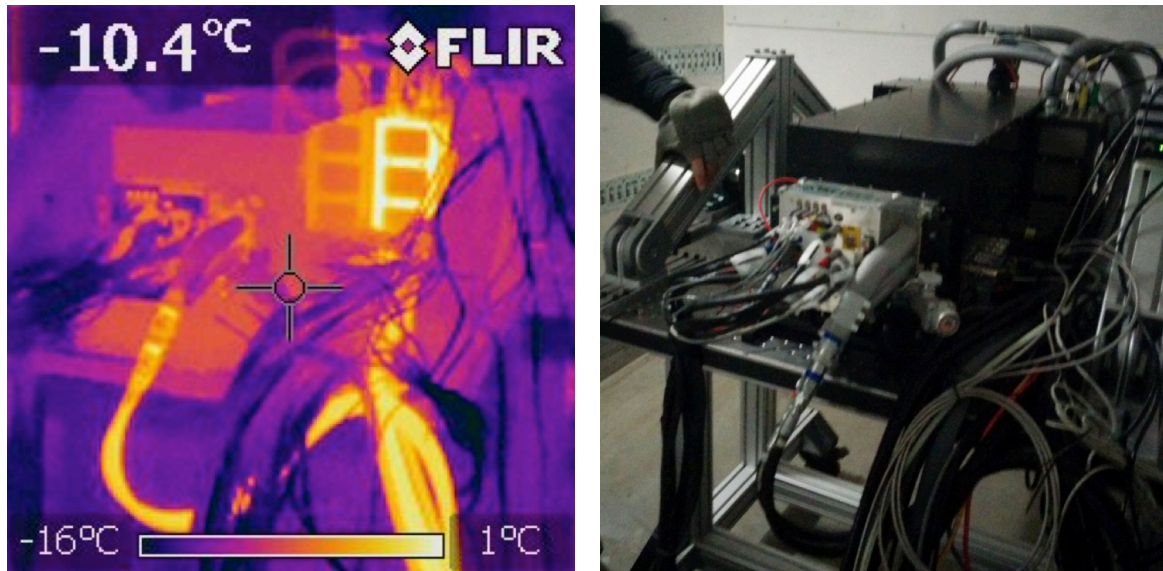


Figure 21 The last part of the WFS Camera pipes, covered with insulating foam is at about -8C; while the non-insulated pipes is much warmer than ambient.

Bottom Line: The thermocamera measurements show that the thermal behavior of the LGSW is generally good. Patrol Cameras and Pockels Cells Drivers require to be insulated.

UPDATE 2014-01-20: Patrol Cameras and Pockels Cell Driver have been shielded with a foam shell and a styrodur case respectively. We assume this is enough to solve the issue. We have no way of repeating the measure of the surfaces temperature in a cold environment now.

25 Appendix C – Closed loop tests with MEMS DM

The DX-LGSW has been provided with a deformable mirror (Boston MEMS 140 actuators) to test the closed loop operation. The MEMS DM operation, foreseen since the design phase (see AD1 Sections 4.3, 5.1.12 and 6.4), has been installed on the external side of the calibration unit.

In addition to that, a lateral panel of the LGSW enclosure was temporarily substituted with one having a glass window that was used to shine the beam coming from the 4D interferometer onto the DM. The reflected beam follows the path back into the 4D and permits to measure the mirror figure. Part of the reflected beam is split and an image is created on an auxiliary camera mimicking the instrument. The auxiliary camera produces the image of the 633nm interferometer beam.

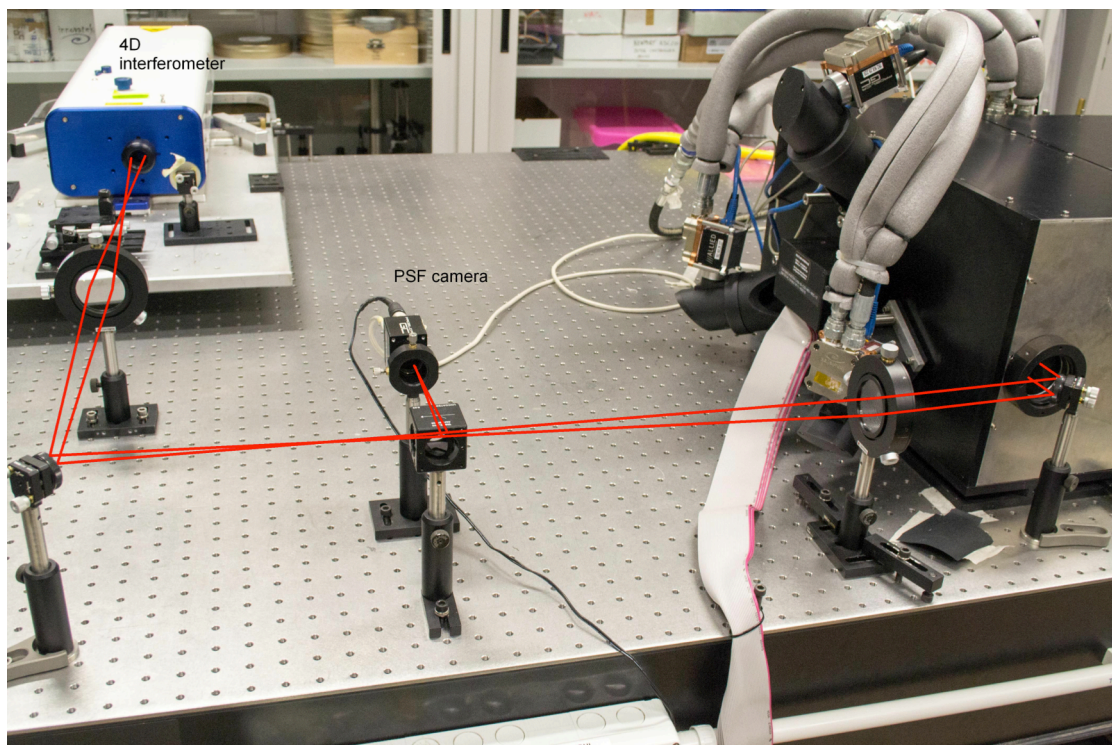


Figure 22 View of the external setup to calibrate the MEMS DM and produce a PSF image

As done for the FLAO tests, the turbulence is injected in the system by superimposing a screen to the closed-loop command. A complete description of the calibration of the ARGOS MEMS DM and its use as atmospheric turbulence generator is given in AD5 that reports on some tests done in 2012 during LGSW integration (without the pnCCD WFS camera).

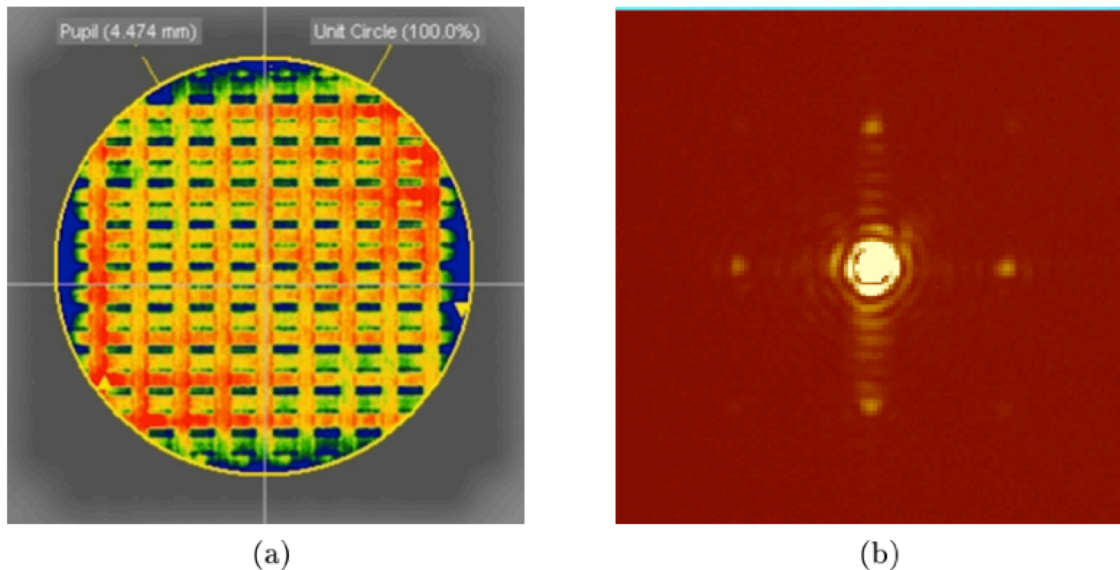


Figure 23 (a) Flattened MEMS surface measured by the 4D. A 4.5 metal diaphragm has been installed to produce a circular pupil. Note the MEMS characteristic actuators footprint creating a rectangular grid. The surface error on the aperture is 22.6nm rms. (b) PSF image on the auxiliary camera for a flattened MEMS. The 4 spots are due to diffraction from the the actuators grid.

The obtained setup is in many respects perfectly similar to what the LGSW will experience at the telescope. The main differences are due to 1) the limited number of actuators of the MEMS DM (the modal base contains only 66 modes) that limit the spectral components of the injected turbulence and 2) the presence of a single turbulent layer conjugated to ground (since the atmosphere is mimicked by the DM itself). These 2 differences make the corrected PSF very different from the expected PSF at the telescope. In fact, the 66-modes reconstructor can correct the entire turbulence spectrum and no high-layer turbulence remains in the path. The bandwidth error being the only residual term (about 40-50nm rms for typical seeing and wind values), the corrected image reaches the diffraction limit.

25.1 Use of MEMS DM to mimic the LBT-ASM

We developed an auxiliary SW suite (integrated into the ARGOS control SW) to mimic with the MEMS DM the operations typically done at the LBT with the ASM.

The software implements the same modal control that is implemented on board of the ASM BCUs (including delay lines, modes2command matrix and superimposition of a “disturb” command) and exposes an interface that is a subset of the AdSec ICE interface that the AARB will use at LBT.

Most important, the software mimics the diagnostic-over-Ethernet feature of the ASM: it creates the UDP diagnostic packets with the same format and content of the “real” ones and streams them over the Ethernet to the dx-lgsworkstation.

This feature allowed the MPIA SW team to develop the BCU diagnostic receiver into the BCU Basdard and test it into its final configuration. The diagnostic receiver is the source for CCD frames, TT commands and slopes for all the needs of LGSW Control SW.

The MEMS software reads the latest slope vector from the LGSW Control SW, reconstructs the wavefront, adds the “disturb”, sends the command to the MEMS DM actuators and finally sends the UDP diagnostic packet to the receiver.

The AO loop can run at speed >100Hz (while the WFS camera is actually running at 1kHz, so 9 out of 10 slope vectors are discarded).

25.2 Interaction Matrix acquisition

The positions of the pupils on the SH lenslet array are fine-tuned using the pupil motors until an optimal illumination is obtained. The current pupil position is stored as “target” of the pupil stabilization loop.

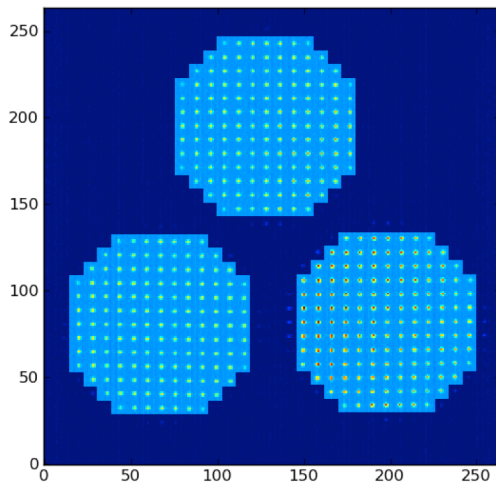


Figure 24 Subaperture definition used with MEMS

The subapertures are then defined to create circular pupils of 13 subapertures on the diameter (instead of 15, because of the reduced diameter of the MEMS mask) see Figure 24. This is a semi-automatic operation: the software selects the subapertures based on their illumination but the AO engineer can decide to remove or add subapertures using the command-line terminal.

An interaction matrix of the 66 modal base was acquired (REFERENCE: 20130926_184400). The temporary algorithm used is a **slow** push-pull, suitable for lab use, but different from the one to be implemented for the use at the telescope. The implementation of the

definitive AO loop calibration routines is outside of the scope of the LGSW Control SW and must be managed at an upper level. The interaction matrix is displayed in Figure 25

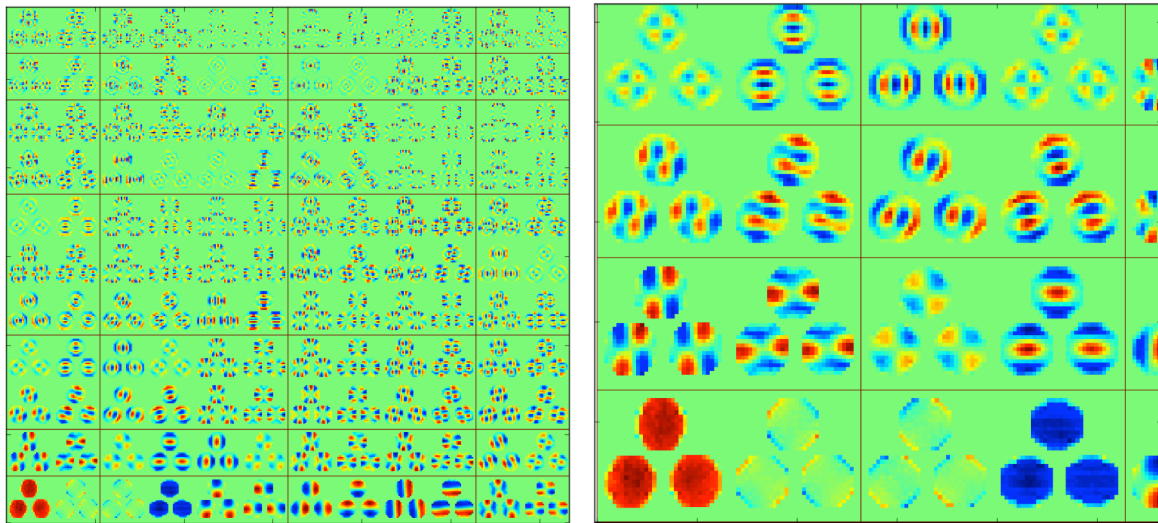


Figure 25 On the left: Interaction Matrix for MEMS DM. In increasing mode number from bottom left (mode 0=tilt) to top right (mode 65). On the right: zoom of the full IM. Visible modes are 0,1,6,7,12,13,18,19.

25.3 WFS measurement noise

A 66 modes reconstructor has been computed from the interaction matrix. Measurement noise is estimated in the following way:

- the system is setup with a given illumination, no atmospheric turbulence and gain=0
- a set of about 1000 slopes is acquired
- the reconstructor is multiplied by the slopes to obtain the modal coefficients of the wavefront
- the temporal variance of the modal coefficient is computed.

The procedure is repeated for different illumination level.

The measurement error for 3 different illumination levels (1000, 400 and 100 photons per subaperture per integration time) is shown in Figure 26.

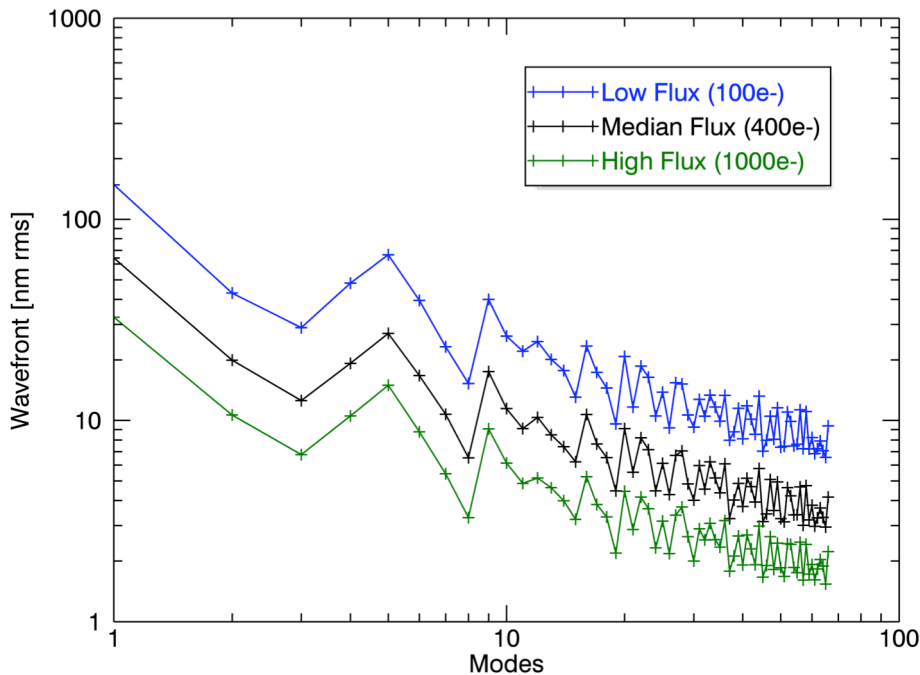


Figure 26 Measurement noise for 3 different levels of illumination. The wavefront (on the 66 modes base) is 47, 91, 210nm rms for high, medium and low flux respectively. This measure has been done in open loop, without turbulence.

REFERENCE: 20131007_121203, 122451, 121239

To extrapolate the total error on a 150 modes base we can assume (being conservative) that all the 84 modes between 66 and 150 have the same noise of mode 66 (about 2nm). Integrating the variances we get an extrapolated wavefront error at 1000ph/subap of

$$WF_{150} = \sqrt{WF_{66}^2 + 2^2 \cdot 84} = 50nm$$

To extrapolate the behavior at the nominal photon flux of 1800 ph/subap we consider that the noise

$$\text{scales as } \sigma = \sqrt{N_{phot} + n_{pixel} RON^2}$$

We assume a Read-Out Noise of 4ph on 64 pixels per subaperture and we obtain a scaling factor

$$\frac{\sigma_{1800}}{\sigma_{1000}} = \sqrt{\frac{1800 + 64 \cdot 16}{1000 + 64 \cdot 16}} = 1.18$$

Hence the wavefront measurement error extrapolated on a 150 mode-base at 1800 ph/subap is 42nm.

25.4 Closed loop performances

The closed-loop tests have been performed with a turbulence of $r_0=10cm$, $L_0=30m$ and wind speed=10m/s (approx. 1" seeing), with tip and tilt removed.

The AO loop was closed on every mode, including tip-tilt. Gain was set to 0.5 for every mode.

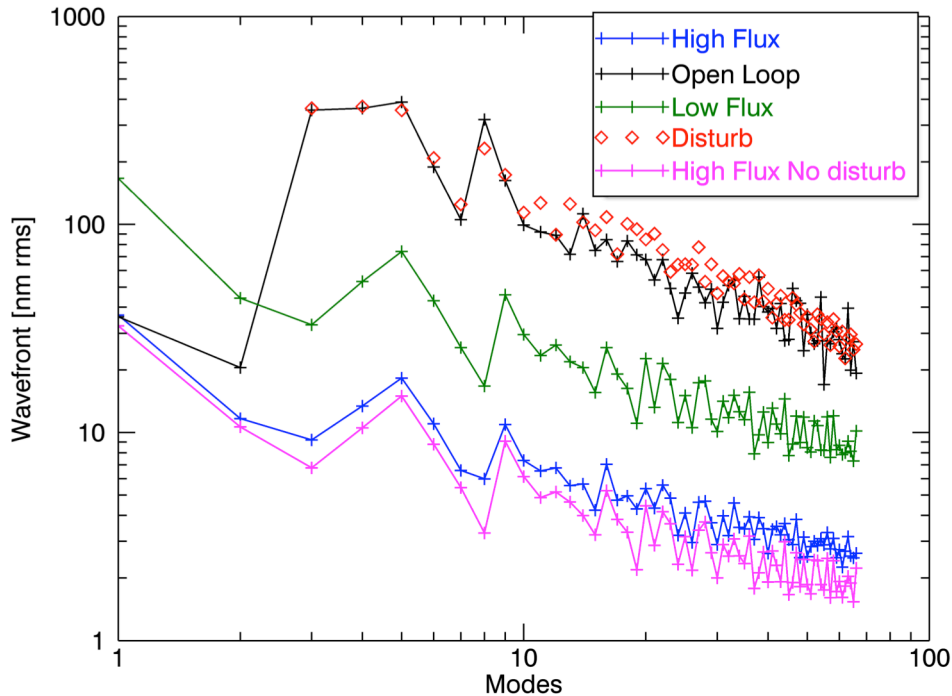


Figure 27 Residual wavefront amplitude after AO correction decomposed on the modal base. Blue: high flux regime (about 1000ph/subap). Green: low flux regime (100ph/subap). Black: open loop. Red: atmospheric turbulence injected as disturb. Magenta: high flux without turbulence. Note that Tip and Tilt are not present in the disturb, but they are used in the reconstructor.

REFERENCE: 20131007_112917, 115050, 120854, 121239

The plot in Figure 26 shows the results obtained. From a comparison of the curves in high flux regime with and without turbulence (blue and magenta) we can estimate the contribution of temporal error. The wavefront error at 1000ph/subap passes from 47nm rms in the no-turbulence case (magenta) to 58nm in the turbulence case (blue).

Assuming that the only added effect is the effect due to temporal delay error that coadds in quadrature to the measurement noise we can estimate the temporal delay error to be 34nm rms, that is consistent with what the theory predict for an AO system running at 1kHz with $r_0=0.1\text{m}$ and wind-speed=10m/s.

Bottom Line: The tests done with the MEMS DM have served as a test-bench of closed loop operation. They allowed developing a basic skeleton for the closed-loop software even if this is not ready for telescope use (and it is outside of LGSW scope). The tests demonstrated that the DX_LGSW is capable of delivering a WF measurement that is in agreement with the specifications.

26 Appendix D - Device list and present configuration

At the date of 30 Jan 2014 the LGSW device list is the following:

Item ID	P/N	Description
Avt Camera #4	02-2130A-06763	VideoCamera
Avt Camera #5	02-2130A-06761	VideoCamera
Avt Camera #6	02-2130A-06760	VideoCamera
Dark Wheel #01	1	Filter wheel
Dark Wheel Motor #01	1	electric motor
Newport NSA12 #00	12941	electric motor
Newport NSA12 #01	13840	electric motor
Newport NSA12 #10	13922	electric motor
Newport NSA12 #11	13854	electric motor
Newport NSA12 #12	13445	electric motor
Newport NSA12 #09	13862	electric motor
PI S334 #1	111012615	piezoelectric driver
PI S334 #2	111012616	piezoelectric driver
PI S334 #3	111012617	piezoelectric driver
Pockels Cell #2	2	opto-electrical shutter
Pockels Cell #3	3	opto-electrical shutter
Pockels Cell #4	4	opto-electrical shutter
Stepper Motor Adaptor Box DX	ADBOX DX	electric interface box
THOR #3	3	T&H internal sensor
THOR #1	1	T&H external sensor
THOR sensor TH01	TH01	sensor
THOR sensor TH04	TH04	sensor
THOR sensor TH17	TH17	sensor
THOR sensor TH24	TH24	sensor
THOR sensor TH27	TH27	sensor
THOR sensor TH30	TH30	sensor
WFS Camera #2	2	Video camera

The running software is version 4102 of the ARGOS software and version 12123 of the TaN software.



27 Appendix E – Spare parts list

List of spare parts to be shipped to LBT with the DX-LGSW

Item ID	QTY	P/N	Description
THOR Unit	1	5	sensors converter
THOR Sensors	13		sensor + cables
Newport NSA12 RED	1		motor
Newport NSA12 BLUE	1		motor
Newport NSA12 YELLOW	1		motor
Avt Camera	1		video camera
Dichroic motor	1	04227	motor
LED Source	1		power supply+led
Dark Wheel Motor	1		motor
WFS parts			
THOR unit	1		sensors converter
THOR sensors	8		sensor + cables
Pockels Cells Driver 2	1		electronic module
Cable Mocon 1	2	W1/5	electrical cable
Piezo-BCU Cable 4	3	PI 4/5/6	electrical cable
Fibers	1		optical fiber
THOR cables	1		electrical cable
Ethernet thor cable	1		ethernet cable
PatrolCamera cable	1		electrical cable
Etherner PatrolCamera cable	1		ethernet cable
Spare cables			
dichroic cables	6		electrical cables
PI cables	2	PI1/2	electrical cables
MoCon cables	2	W6/7	electrical cables
THOR cables	1	THOR3	power cable
Fiber	1		optical fiber

28 List of acronyms

AARB	ARGOS Arbitrator
AGW	Acquisition Guiding and Wavefront sensing
AIP	Astrophysical Institute Potsdam
AOS	Adaptive Optics System
APD	Avalanche Photo Diode
ASM	Adaptive Secondary Mirror
BCU	Basic Computational Unit
DM	Deformable Mirror
DMD	Deformable Mirror Diagnostics
FLAO	First Light Adaptive Optics
FWHM	Full Width Half Maximum
GLAO	Ground Layer Adaptive Optics
IDL	Interactive Data Language
IIF	Instrument InterFace
LBT	Large Binocular Telescope
LBTO	LBT Observatory
LGS	Laser Guide Star
LGSF	LGS Facility
LGSW	LGS Wavefront Sensor
	LBT Near Infrared Spectroscopic Utility with Camera and Integral Field Unit for
LUCI	Extragalactic Research
MPE	Max-Planck-Institut für extraterrestrische Physik
MPIA	Max-Planck-Institut für Astronomie
NGS	Natural Guide Star
OAA	Osservatorio Astrofisico di Arcetri
PID	Proportional, Integral and Differential
PSF	Point Spread Function
RLGS	Rayleigh Laser Guide Star
RMS	Root Mean Square
RON	Read Out Noise
RPC	Remote Procedure Call
RTC	Real Time Control
SH	Shack Hartmann
SNR	Signal to Noise Ratio
SR	Strehl Ratio
SVD	Single Value Decomposition
TaN	Twice as Nice common software developed in MPIA
TBC	To Be Confirmed
TBD	To Be Defined
TCS	Telescope Control Software
TT	Tip Tilt
TTW	Tip Tilt Wavefront sensor
WFS	WaveFront Sensor



DX-LGSW integration report

Doc: ARGOS Tech Note 120
Issue 2
Date 30/01/2014
Page 50 of 50

End of document